



LIGO Laboratory / LIGO Scientific Collaboration

LIGO- T1000747-v3

LIGO

01/6/11

AOS SLC Arm Cavity Baffle FDR

Michael Smith, Virginio Sannibale, Niem Nguyen

Distribution of this document:
LIGO Scientific Collaboration

This is an internal working note
of the LIGO Laboratory.

California Institute of Technology
LIGO Project – MS 18-34
1200 E. California Blvd.
Pasadena, CA 91125
Phone (626) 395-2129
Fax (626) 304-9834
E-mail: info@ligo.caltech.edu

Massachusetts Institute of Technology
LIGO Project – NW22-295
185 Albany St
Cambridge, MA 02139
Phone (617) 253-4824
Fax (617) 253-7014
E-mail: info@ligo.mit.edu

LIGO Hanford Observatory
P.O. Box 159
Richland WA 99352
Phone 509-372-8106
Fax 509-372-8137

LIGO Livingston Observatory
P.O. Box 940
Livingston, LA 70754
Phone 225-686-3100
Fax 225-686-7189

<http://www.ligo.caltech.edu/>

Table of Contents

1	<i>INTRODUCTION</i>	7
1.1	Final Design Review Checklist	7
1.1.1	Final requirements – any changes or refinements from PDR?	7
1.1.2	Resolutions of action items from SLC PDR.....	7
	ISI “0” (HEPI) motion	7
	Lower BRDF Material for Baffles	7
	Viton O-Ring Suspension	7
	Suspension Internal Modes	7
	Earthquake Stops	7
	Un-baffled Light	8
	Shape of Arm Cavity Baffle	8
1.1.3	Subsystem block and functional diagrams.....	8
1.1.4	Final Parts Lists and Drawing Package (assembly drawings and majority of remaining drawings)	8
1.1.5	Final specifications	8
1.1.6	Final interface control documents.....	8
1.1.7	Relevant RODA changes and actions completed	8
1.1.8	Signed Hazard Analysis.....	8
1.1.9	Final Failure Modes and Effects Analysis	9
1.1.10	Risk Registry items discussed.....	9
1.1.11	Design analysis and engineering test data	9
1.1.12	Software detailed design	9
1.1.13	Final approach to safety and use issues	9
1.1.14	Production Plans For Acquisition Of Parts, Components, Materials Needed For Fabrication	9
1.1.15	Installation Plans and Procedures	9
1.1.16	Final hardware test plans	9
1.1.17	Final software test plans	9
1.1.18	Cost compatibility with cost book	9
1.1.19	Fabrication, installation and test schedule	10
1.1.20	Lessons Learned Documented, Circulated	10
1.1.20.1	Porcelainizing	10
1.1.20.2	Clamping to Stage 0.....	10
1.1.21	Problems and concerns	10
1.2	Applicable Documents	10
2	<i>ARM CAVITY BAFFLE CONFIGURATIONS</i>	11
2.1	L1 Interferometer	11
2.2	H1 Interferometer	12
2.3	H2 Interferometer	13
3	<i>DESCRIPTION OF THE ARM CAVITY BAFFLE</i>	15
3.1	Baffle Assembly	15

3.1.1	Requirement to Lift the ACB Out of the Way while Working on Quad Suspension...	18
3.1.2	Earthquake Stops	19
3.2	Arm Cavity Baffle Suspension.....	20
3.2.1	Transmissibility Measurements	20
3.2.2	Stray Magnetic Field Measurement.....	22
3.2.3	LASTI Arm Cavity Baffle Suspension Test.....	23
3.3	ALS Photo detector Array	23
3.3.1	Light Power on the ALS Photo detector	26
4	SCATTERED LIGHT DISPLACEMENT NOISE	28
4.1	Arm Cavity Baffle Surface.....	28
4.1.1	Arm Cavity Baffle Surface Scatter	28
4.2	Scattered Light Displacement Noise from ALS Photo detector Array.....	30
4.3	Scattered Light Calculation Parameters	30
4.4	Scattering from Main Arm Beam.....	31
4.4.1	Power Hitting Photo detector Surface and Screw Head	31
4.4.2	Power Scattered into IFO Mode	32
4.4.2.1	Scattering by Photo detector	32
4.4.2.2	Scattering by Screw Head.....	33
4.4.3	Displacement Noise	33
4.5	Scattering from COC Scattered Light.....	33
4.5.1	Power Hitting Photo detector Surface and Screw Head	33
4.5.2	Power Scattered into IFO Mode	33
4.5.2.1	Scattering by Photo detector	33
4.5.2.2	Scattering by Screw Head.....	34
4.5.3	Displacement Noise	34
5	INTERFACES	35
5.1	Interface to ITM and ETM Mirrors	35
5.2	Stay Clear Margin	41
5.3	Electrical Interfaces.....	41

Table of Figures

<i>Figure 1: L1 Arm Cavity Baffle Configuration</i>	<i>12</i>
<i>Figure 2: H1 Arm Cavity Baffle Configuration.....</i>	<i>13</i>
<i>Figure 3: H2 Arm Cavity Baffle Configuration.....</i>	<i>14</i>
<i>Figure 4: 2-Hole Arm Cavity Baffle Assembly.....</i>	<i>15</i>
<i>Figure 5: 1-Hole Right, Arm Cavity Baffle Assembly</i>	<i>16</i>
<i>Figure 6: 1-Hole Left, Arm Cavity Baffle Assembly.....</i>	<i>17</i>
<i>Figure 7: Arm Cavity Baffle Rotated Away from the Quad Suspension.....</i>	<i>19</i>
<i>Figure 8: Earthquake Stops.....</i>	<i>20</i>
<i>Figure 9: ALS Photodiodes Mounted to Back Side of ACB.....</i>	<i>24</i>
<i>Figure 10: ALS Photo detector Assembly.....</i>	<i>25</i>
<i>Figure 11: ALS Photo detector Cabling.....</i>	<i>26</i>

Figure 12: View toward the ALS Photo detector Array through the Manifold Cryopump Baffle Aperture 27

Figure 13: ARM CAVITY BAFFLE SCATTER..... 28

Figure 14: Measured BSC ISI Stage 0, LLO 29

Figure 15: Scattered Light Displacement Noise from Arm Cavity Beam, and from the COC Scattered Light..... 35

1 INTRODUCTION

1.1 Final Design Review Checklist

1.1.1 Final requirements – any changes or refinements from PDR?

[T070061-v1-D Stray light Control Design Requirements](#), was revised to add the requirement for a photo detector array around ACB opening for assisting in the initial pointing of the Arm Length Stabilization beams.

1.1.2 Resolutions of action items from SLC PDR

Refer to: LIGO-L0900119-v1

ISI “0” (HEPI) motion

Please assess the stray light noise estimates with these more realistic inputs for those items being attached to the BSC ISI stage 0.

Ans: See 4

How much isolation is needed for each of the six DOF? Has the proposed design been evaluated for each of these DOF?

Ans: The design was evaluated for the horizontal DOF, which is the worst case.

Lower BRDF Material for Baffles

We suggest the team consider a lower-BRDF material for the more critical baffles, and in particular suggest looking at the electro-static frit black-enameled steel as an option that would give better optical performance.

Ans: We will use black porcelainized steel baffles; See 4.

Viton O-Ring Suspension

Review the tests that have been carried out with the Viton o-ring suspension (is there a report available?).

Ans: The o-ring suspension has been replaced with a maraging steel blade spring that suspends the Baffle from a flexible wire. The baffle is damped with eddy-current damping magnets moving against a fixed copper plate mounted to the down tube of the suspension assembly.

Suspension Internal Modes

•Anything connected to ISI stage 0 should be as light as possible and have body modes no higher than several Hertz (to avoid being problematic for the ISI controls). We suspect the o-ring mount proposed is too stiff in some degrees-of-freedom. Have you considered a multi-wire suspension instead, using coil springs, e.g., for vertical compliance? (seems to us something like this would be easier to install and adjust as well)

Ans: The pendulum mode of the suspended baffle is 1.6 Hz. The internal mode of the suspension structure that is mounted to the ISI stage 0 is > 30 Hz; see 3.2.2.

Earthquake Stops

Tell us more about how the EQ stops are to be mounted to the chamber.

Ans: The earthquake stops consist of travel-limiting rods mounted to the large down-tube that holds the eddy-current copper damping plates, which mounts to the ISI Stage 0--see 3.1.2. The rods restrain the motion of the suspended baffle in three axes.

Un-baffled Light

What happens to the scattered light that passes between the arm cavity baffle ID and the OD of the test mass?

Ans: This annular beam of scattered light is allowed to scatter from the SUS structure and eventually from the chamber walls. It will not cause excessive displacement noise.

Shape of Arm Cavity Baffle

Given the round shapes of the test masses and the manifolds, is there merit to a round arm cavity baffle, rather than square?

Ans: No. The efficient light trapping by the louver shape of the baffle structure requires a rectangular shape.

1.1.3 Subsystem block and functional diagrams

See section 2.

1.1.4 Final Parts Lists and Drawing Package (assembly drawings and majority of remaining drawings)

[E1000674 AdLIGO ASO BOM SLC Arm Cavity Baffle Box Final Assy-v1](#)

[E1000880 BOM ACB 1 hole left no QPD](#)

[E1000879 BOM ACB 1 hole right no QPD](#)

[E1000878 BOM ACB 1 hole left QPD](#)

[E1000877 BOM ACB 1 hole right QPD](#)

1.1.5 Final specifications

[E1000083-v4 Spec for Enameled Steel Sheet](#)

[E0900023-v10 Manufacturing Process Spec for Cantilever Spring Blades](#)

[E0900364-v7 LIGO Metal in Vacuum](#)

1.1.6 Final interface control documents

[E1000404-v1 ACB Interface in BSC Chambers H1, H2 for Advanced LIGO\(2\)](#)

[D1002870, Flange Layout, Cable Lengths, Bracket Location and Related Input Documents](#)

[D1002870, Flange Layout, Cable Lengths, Bracket Location and Related Input Documents](#)

1.1.7 Relevant RODA changes and actions completed

Not applicable

1.1.8 Signed Hazard Analysis

[E1000890-v1 ACB Hazard Analysis](#)

1.1.9 Final Failure Modes and Effects Analysis

Not Required

1.1.10 Risk Registry items discussed

None for this subsystem

1.1.11 Design analysis and engineering test data

See 3.2.1 and 3.2.2.

1.1.12 Software detailed design

Not applicable, ISC will handle this.

1.1.13 Final approach to safety and use issues

No operational safety issues

1.1.14 Production Plans For Acquisition Of Parts, Components, Materials Needed For Fabrication

[E1000891-v1 ACB production plan.](#)

1.1.15 Installation Plans and Procedures

This will be deferred until after FDR

1.1.16 Final hardware test plans

- Tests of porcelainized witness samples: ball drop test, visual inspection

Witness samples taken during each furnace run for porcelainizing the baffle parts will be subjected to a visual inspection and to a standard ball drop test to determine if the adhesion of the porcelain material is sufficient.

- FTIR tests of as-porcelainized parts

A representative selection of porcelainized baffle parts from each furnace run will be swabbed and a proper FTIR sample collected for subsequent contamination evaluation.

- Blade stiffness measurement

See [E1000892-v1 Fabrication, Installation, and Test Plan](#)

- Suspended baffle balancing before installation

See [E1000892-v1 Fabrication, Installation, and Test Plan](#)

1.1.17 Final software test plans

Not applicable, ISC will handle this.

1.1.18 Cost compatibility with cost book

See [E1000891-v1 ACB production plan.](#)

1.1.19 Fabrication, installation and test schedule

See [E1000892-v1 Fabrication, Installation, and Test Plan](#)

1.1.20 Lessons Learned Documented, Circulated

1.1.20.1 Porcelainizing

In order to maintain the flatness and avoid warping of flat porcelainized parts during the baking process in the continuous feed furnace, the parts must be suspended in such a way that the forces of gravity act in the plane of the part.

Fabricated non-planar shapes that have structural integrity are best porcelainized by using a stationary furnace, and placing the pieces so that gravity forces act normal to a plane of symmetry.

1.1.20.2 Clamping to Stage 0

Based on past experience of clamping suspension structures to support tables and FEA models, we believe that the Arm Cavity Baffle upper mounting plate should be clamped to the ISI Stage 0 with as many clamps as feasible, the clamps being as close to the center of the large down-tube for the suspension structure as possible.

1.1.21 Problems and concerns

TBD

1.2 Applicable Documents

[E1000674 AdLIGO ASO BOM SLC Arm Cavity Baffle Box Final Assy-v1](#)

[D1002870, Flange Layout, Cable Lengths, Bracket Location and Related Input Documents](#)

[E0900023-v10 Manufacturing Process Spec for Cantilever Spring Blades](#)

[E0900364-v7 LIGO Metal in Vacuum](#)

[E1000083-v4 Spec for Enameled Steel Sheet](#)

[E1000404-v1 ACB Interface in BSC Chambers H1, H2 for Advanced LIGO\(2\)](#)

[E1000890-v1 ACB Hazard Analysis](#)

[E1000891-v1 ACB production plan](#)

[E1000892-v1 Fabrication, Installation, and Test Plan](#)

[T060073-00 Transfer Functions of Injected Noise](#)

[T070061-v1-D Stray light Control Design Requirements](#)

[T080064-00 Controlling Light Scatter in Advanced LIGO](#)

[T0900269-v2 Stray Light Control \(SLC\) Preliminary Design](#)

[T1000738 SLC Suspension, Magnetic Field Measurements of the Eddy Current Damper](#)

2 ARM CAVITY BAFFLE CONFIGURATIONS

Table 1: Arm Cavity Baffle Configurations

IFO	chamber	number of holes	hole location (viewed toward COC)	No of ALS QPDs	no of shielded cables	no of wires per cable	total no of signal wires	no of ground connections	total no of vacuum feed through
H1	BSC1	1	right	0					0
	BSC3	1	left	0					0
	BSC9	2	both	8	2	12	24	2	26
	BCC10	2	both	8	2	12	24	2	26
H2	BSC7	2	both	8	2	12	24	2	26
	BSC8	2	both	8	2	12	24	2	26
L1	BSC1	1	right	4	1	12	12	1	13
	BSC3	1	left	4	1	12	12	1	13
	BSC4	1	right	4	1	12	12	1	13
	BCC5	1	left	4	1	12	12	1	13

2.1 L1 Interferometer

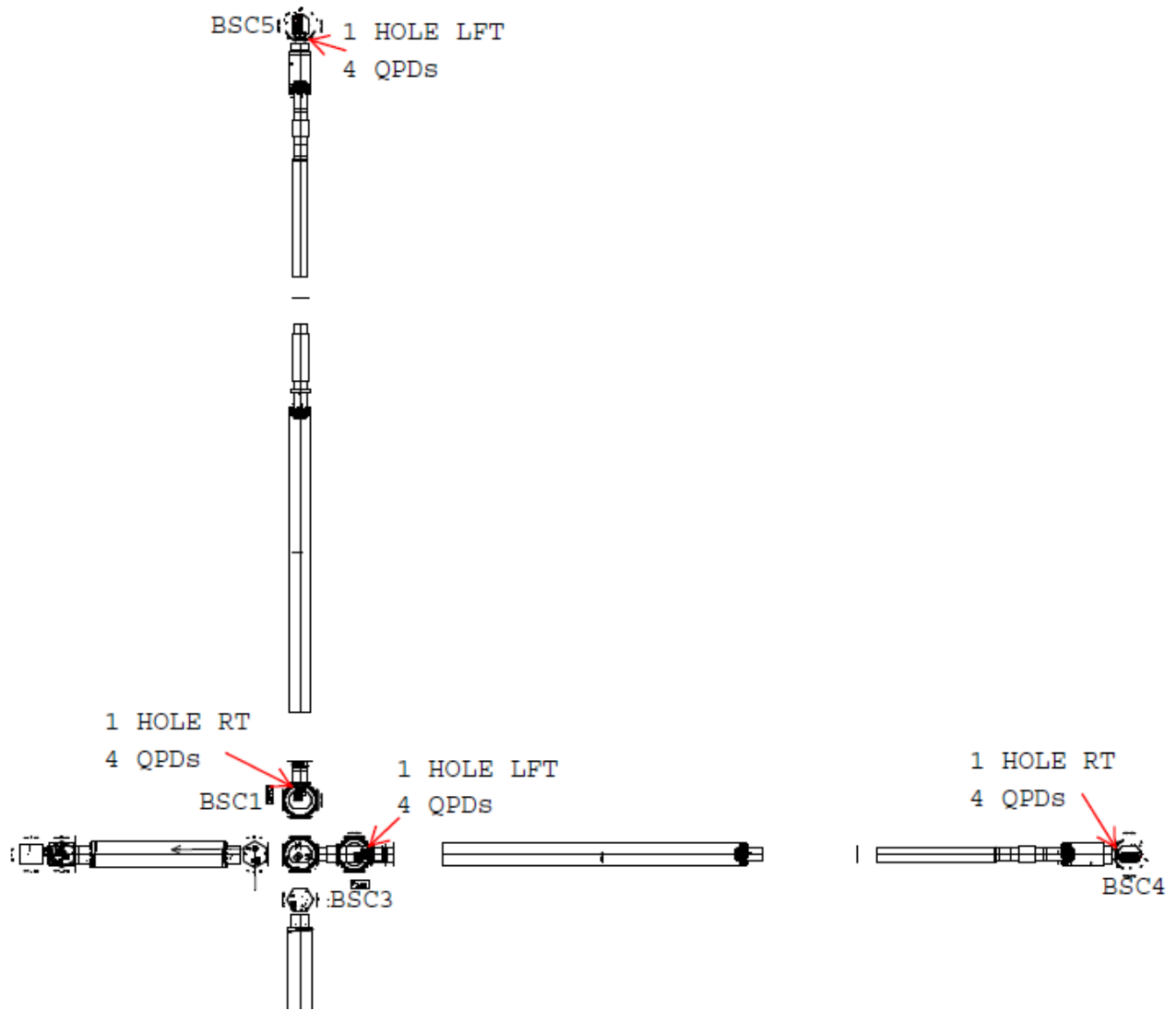


Figure 1: L1 Arm Cavity Baffle Configuration

2.2 H1 Interferometer

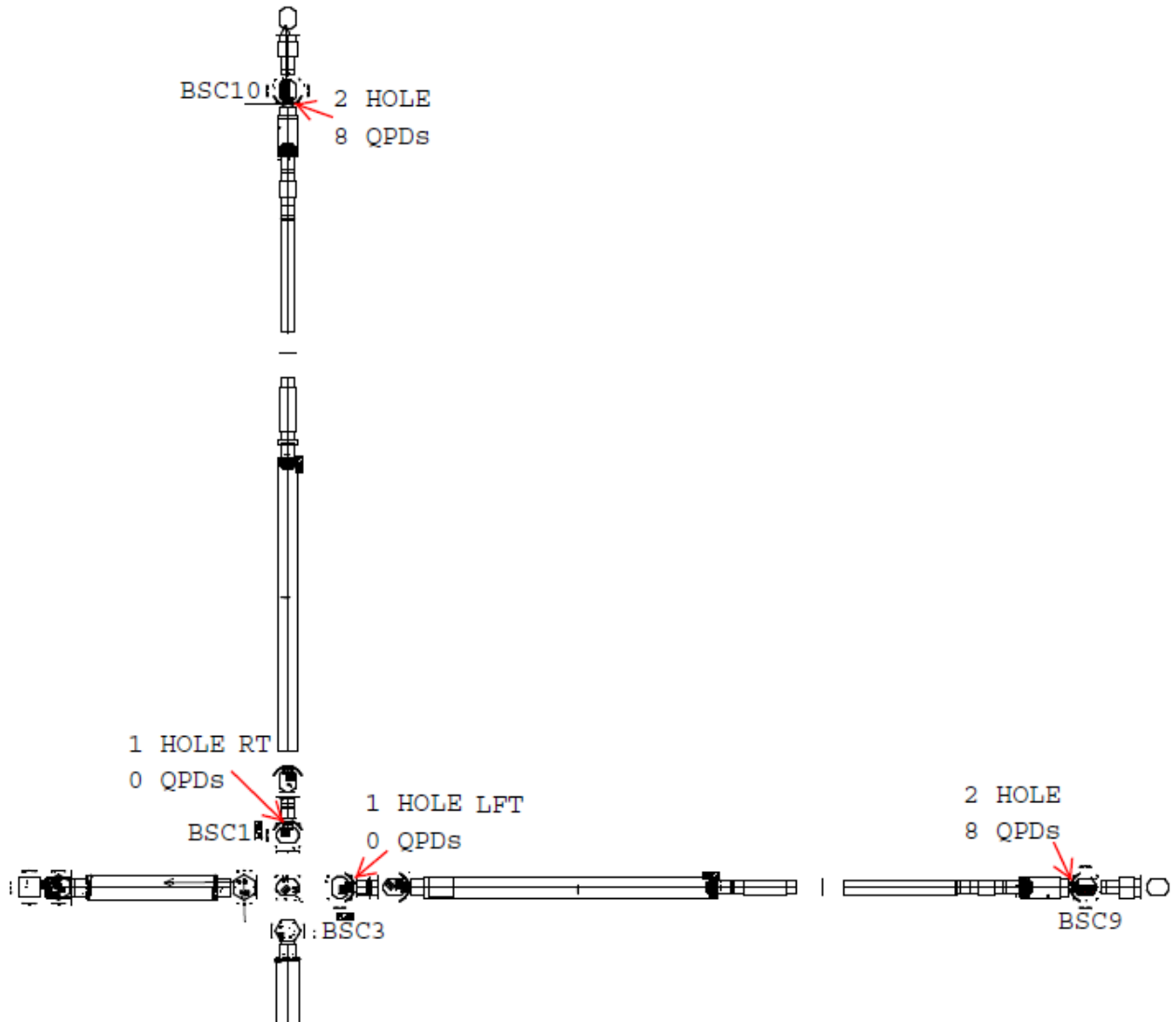


Figure 2: H1 Arm Cavity Baffle Configuration

2.3 H2 Interferometer

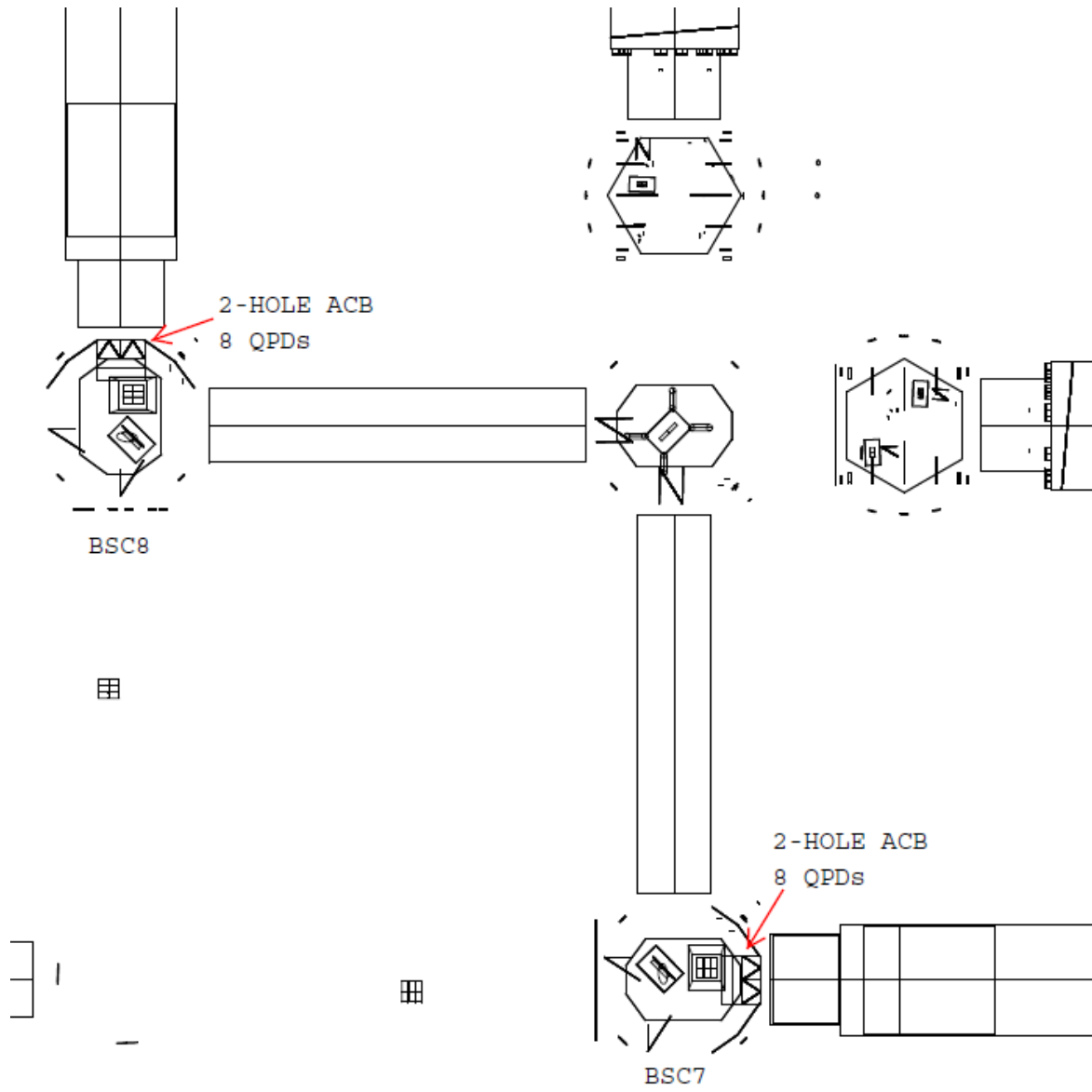


Figure 3: H2 Arm Cavity Baffle Configuration

3 DESCRIPTION OF THE ARM CAVITY BAFFLE

3.1 Baffle Assembly

The suspended Arm Cavity Baffle support plate mounts to the ISI Stage 0 in the BSC chamber. The down tube supports the eddy current damping mechanism. The light-trapping louver structure is made of porcelainized enameling steel. The hole diameters in the baffle are slightly larger than the diameter of the ITM and ETM mirrors.

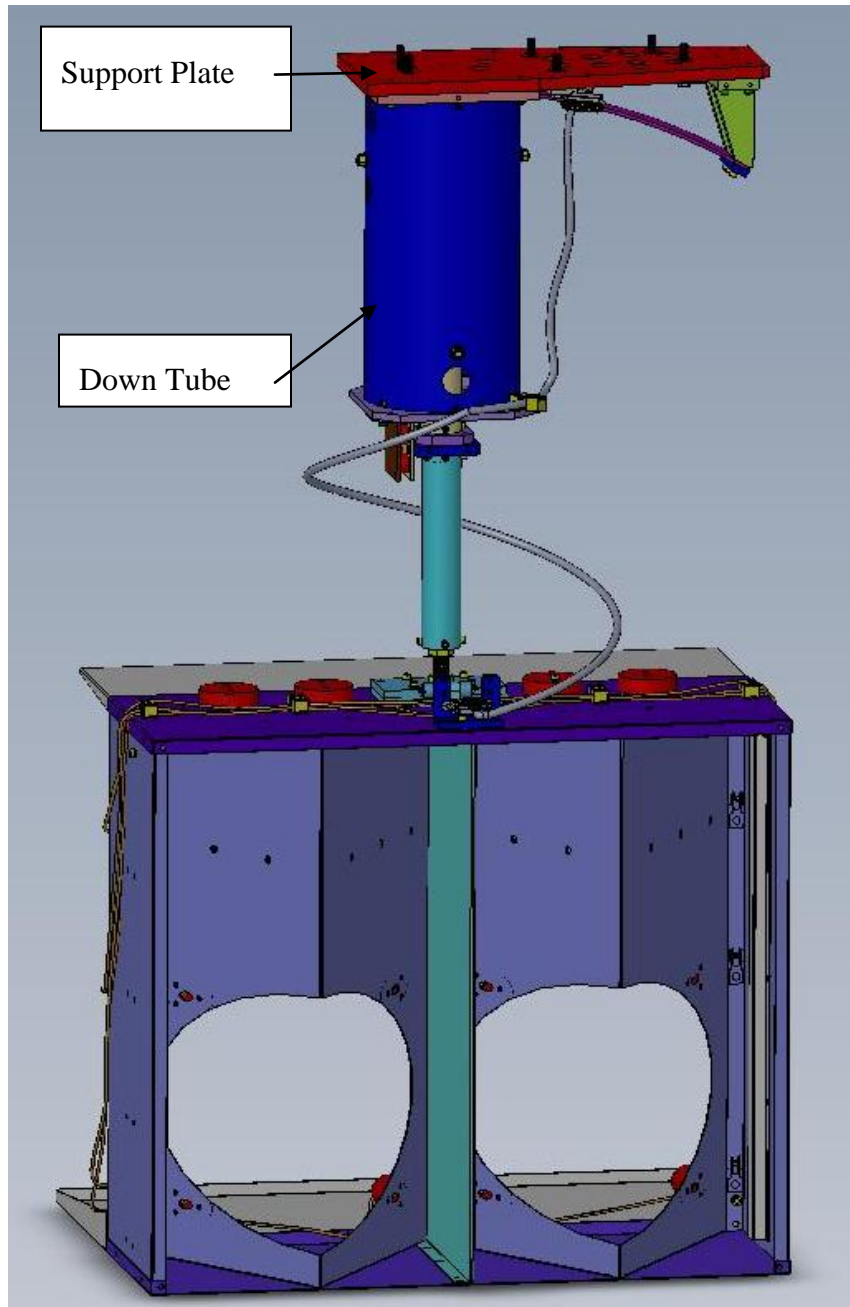


Figure 4: 2-Hole Arm Cavity Baffle Assembly

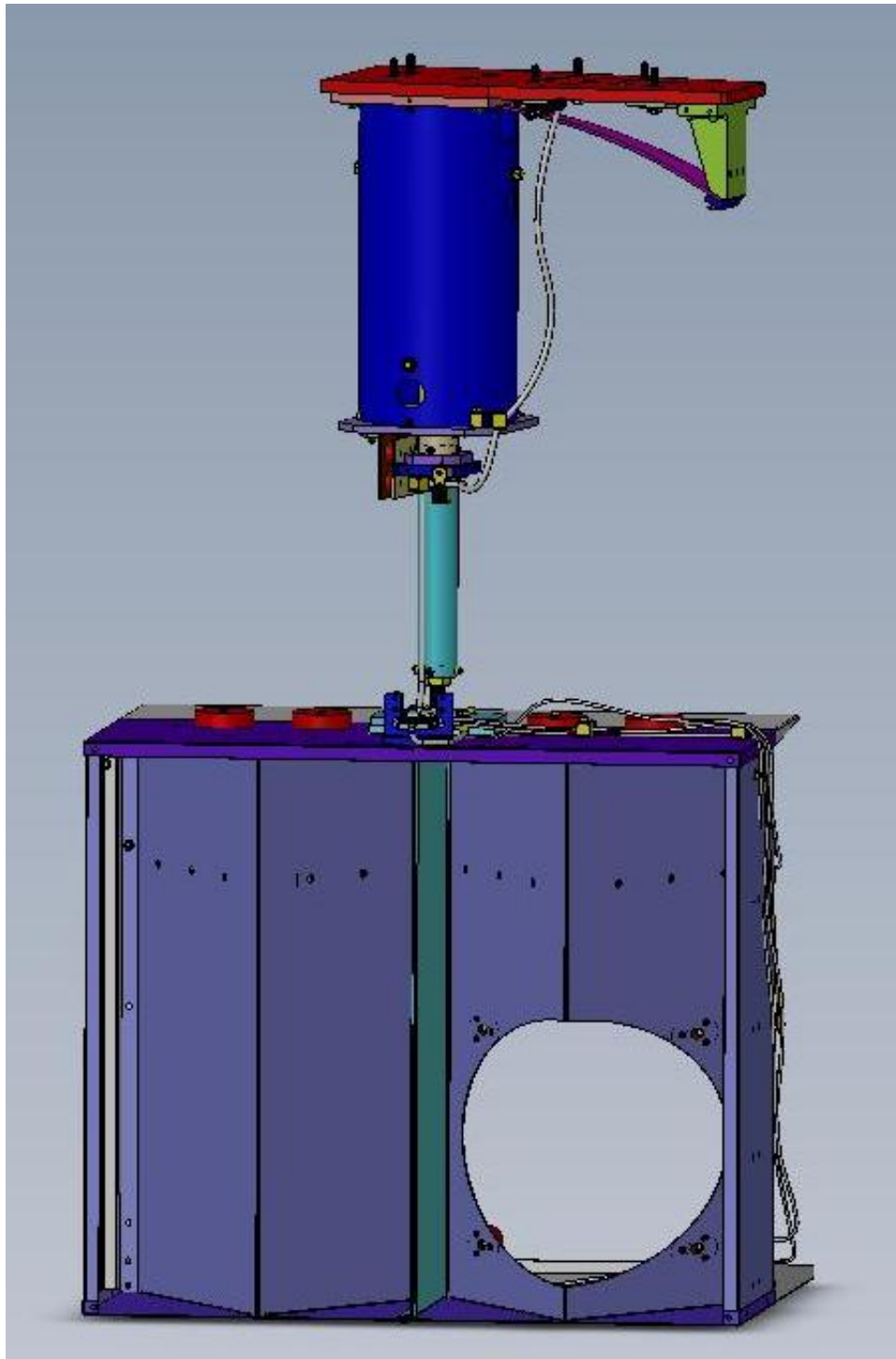


Figure 5: 1-Hole Right, Arm Cavity Baffle Assembly

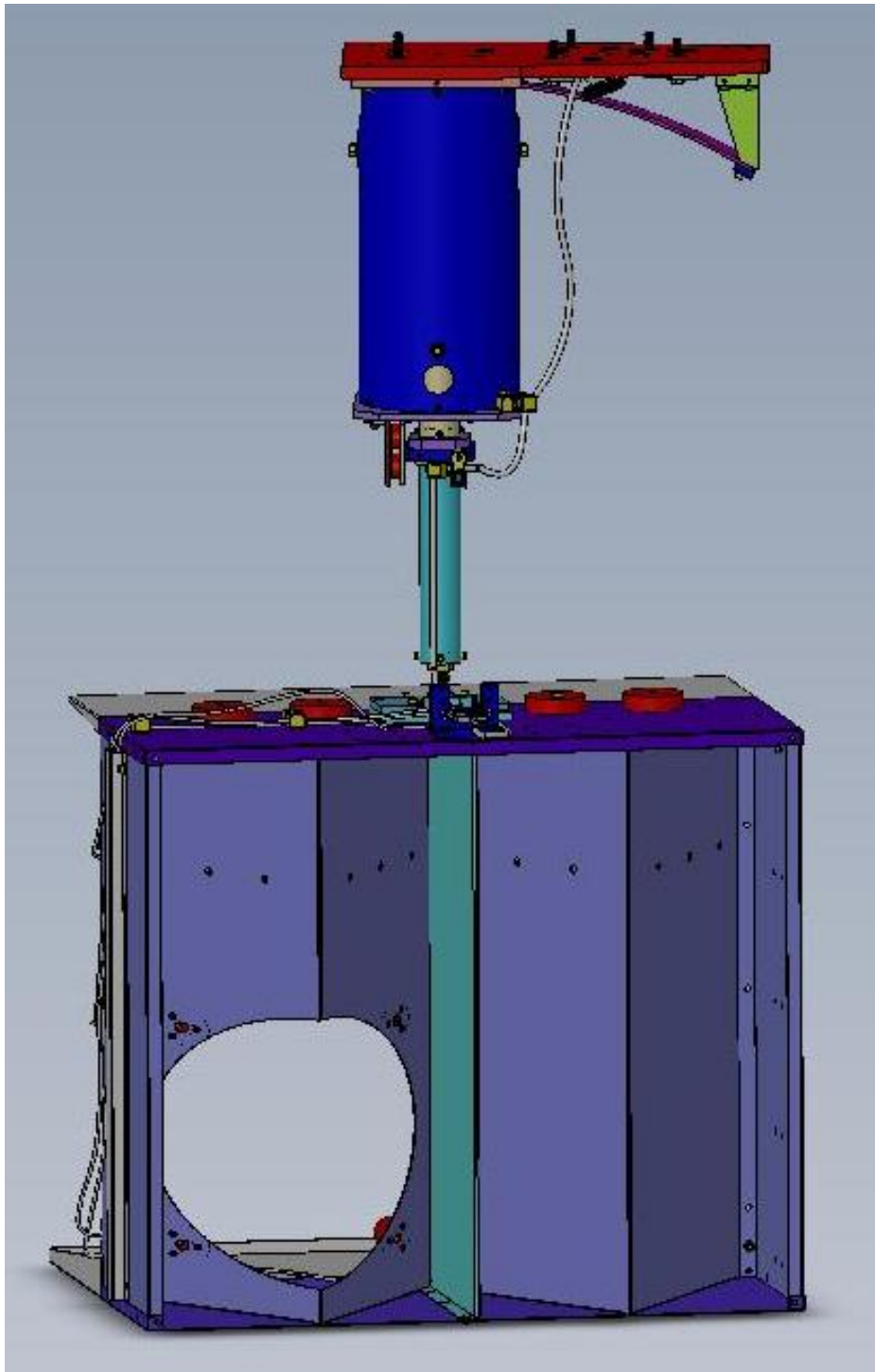


Figure 6: 1-Hole Left, Arm Cavity Baffle Assembly

Table 2: Arm Cavity Baffle Characteristics

Parameter	Value
Aperture diameter	346 mm
Outer diameter blockage	>850 mm
Material	Oxidized polished stainless steel
BRDF	$<0.05 \text{ sr}^{-1}$
Reflectivity	<0.05
Total weight	60 kg
Suspended weight	40 kg

Table 3: Arm Cavity Baffle Suspension

Parameter	Value
Frame	Aluminum frame
Suspension	Two wire, suspended from HEPI stage “0”
Amplitude response	See 3.2.1
Damping	$Q < 100$

3.1.1 Requirement to Lift the ACB Out of the Way while Working on Quad Suspension

The Arm Cavity Baffle attaches to the suspension tube with a hinge joint that allows the baffle to be swung away from the quad suspension structure whenever close access to the COC mirror is needed. The wide-angle baffle plates that protrude like shelves from the arm cavity baffle can also be temporarily removed for additional access to the COC mirror.

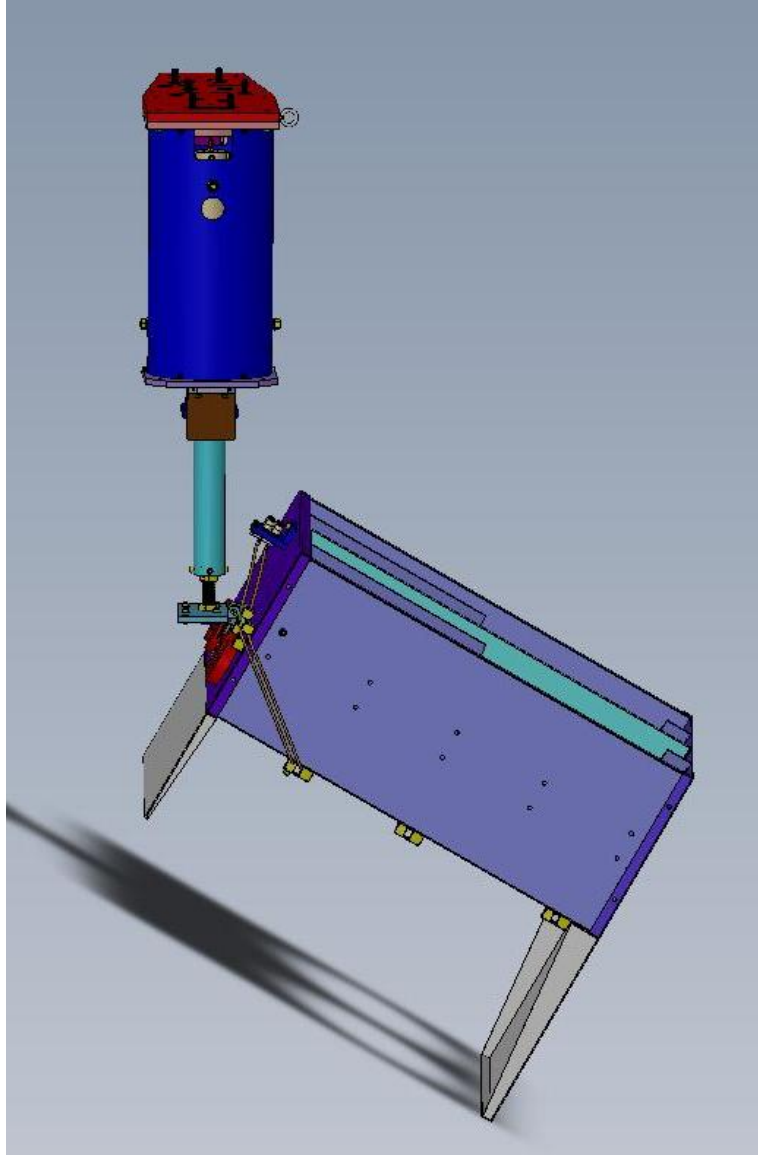


Figure 7: Arm Cavity Baffle Rotated Away from the Quad Suspension

3.1.2 Earthquake Stops

The earthquake stops consist of travel-limiting rods mounted to the large down-tube that holds the eddy-current copper damping plates, which mount to the ISI Stage 0, as shown in Figure 8. The rods restrain the excess motion of the suspended baffle in three axes.

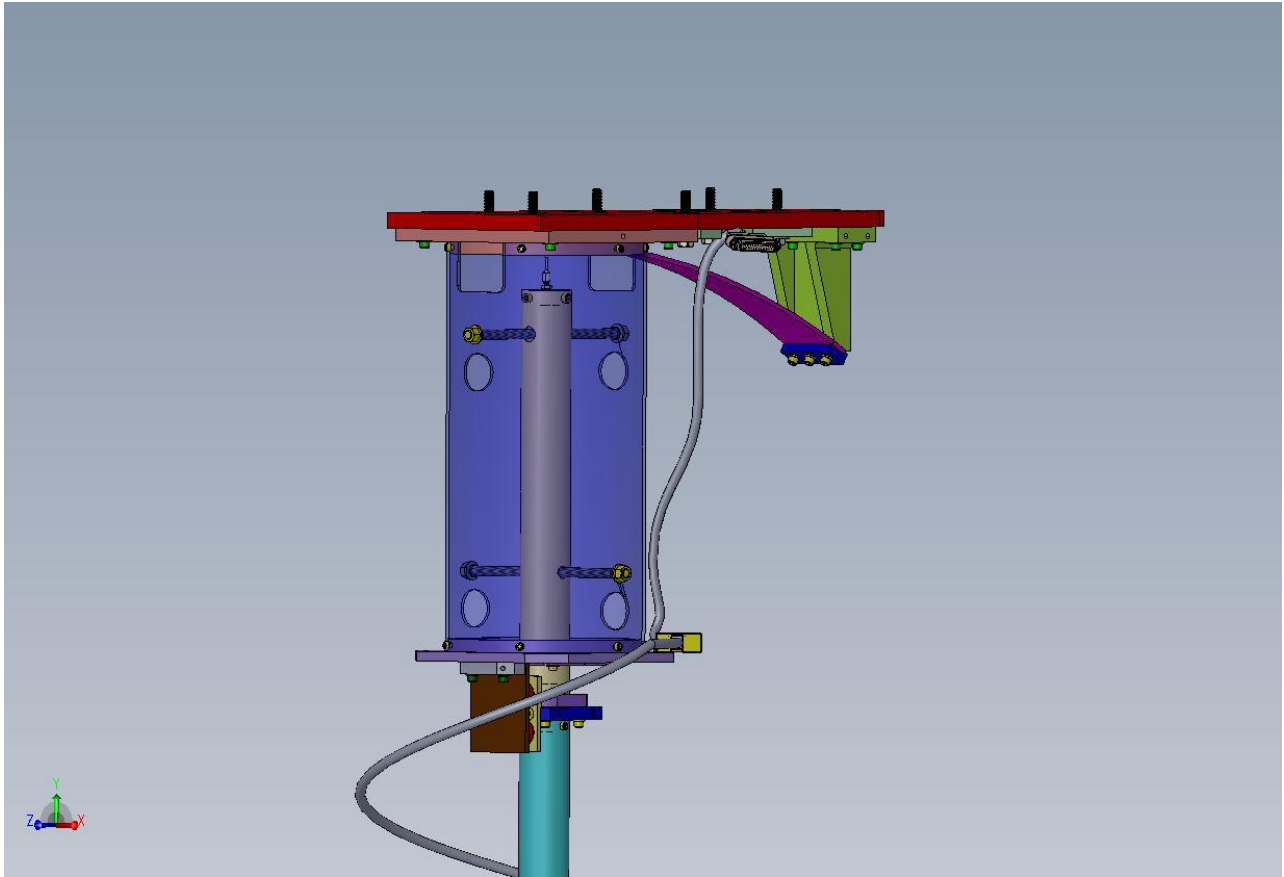
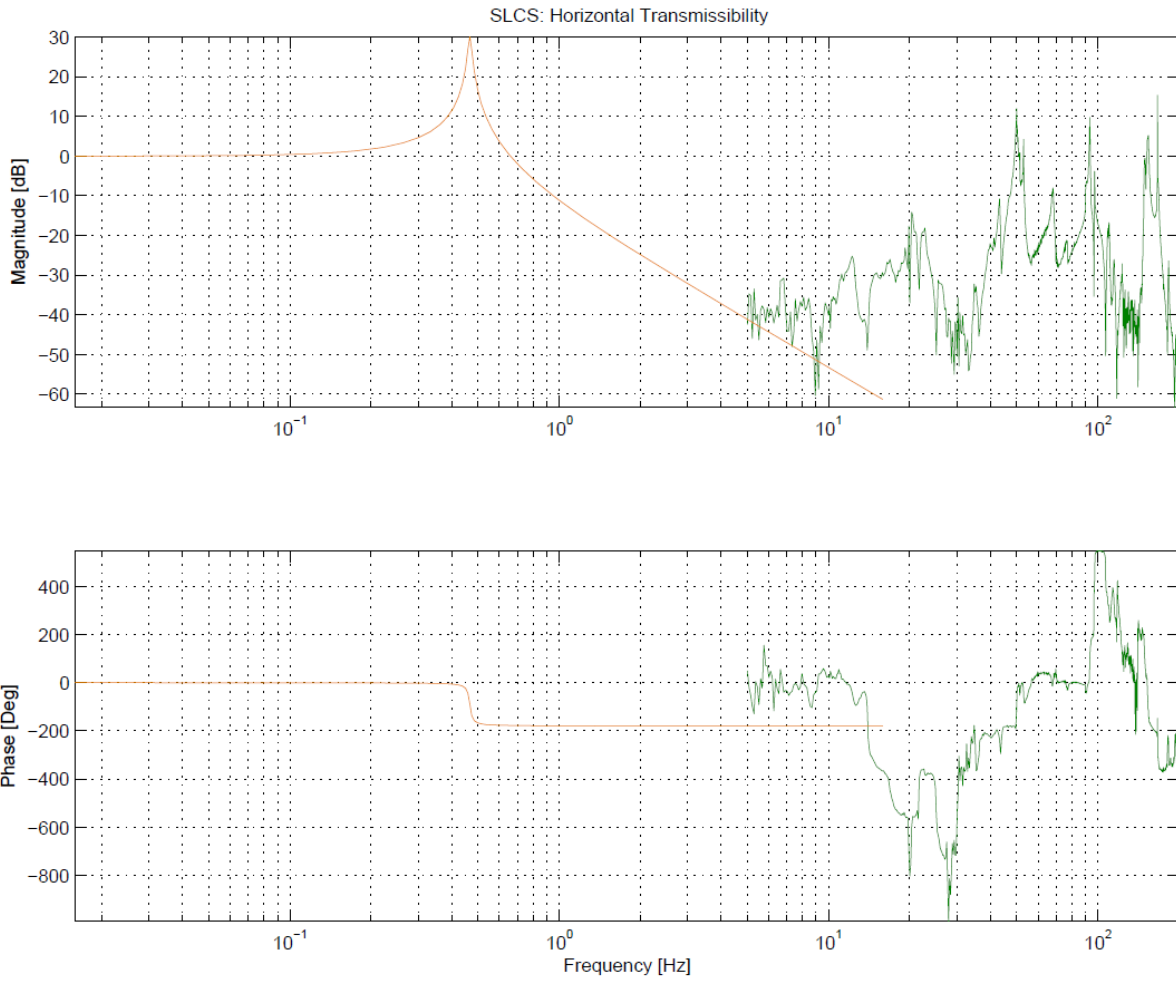


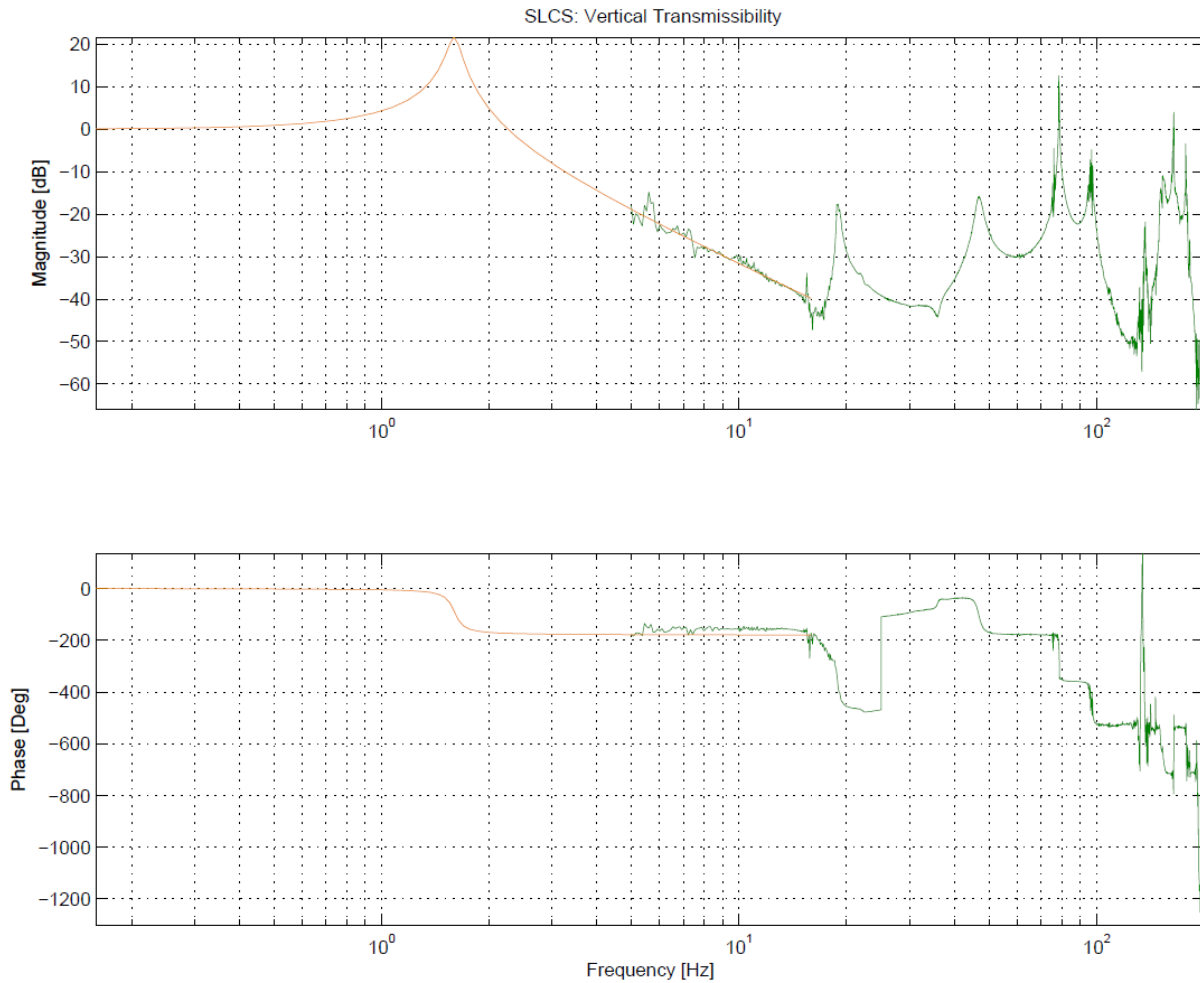
Figure 8: Earthquake Stops

3.2 Arm Cavity Baffle Suspension

3.2.1 Transmissibility Measurements

The measured transmissibilities (green curve) are compared with the damped pendulum analytical model (red curve) in the vicinity of 10 Hz. The actual magnitudes agree reasonably well with the model. Beyond 10 Hz, the amplitude remains approximately constant at the background noise level, except for internal resonances of the baffle suspension.





3.2.2 Stray Magnetic Field Measurement

The eddy current damper magnets of the Arm Cavity Baffle will be placed within approximately 0.5 m of the magnets of the core optic. The interaction of the eddy current damping magnets with the COC suspension magnets was estimated, as described below.

The DC and the frequency spectrum of the stray magnetic field produced by the eddy current damper permanent magnet pairs was. Extrapolations of the stray magnetic field from the measured fits show that the DC magnetic field at a distance of 0.5 m is approximately $1e-17$ T, a value $<$ the earth's natural magnetic field. The magnetic field spectrum measured in the CIT lab is about 8 orders of magnitude lower than the magnetic field spectrum measured at the Hanford site ($1e-11$ T/rtHz,) even though the seismic noise at CIT is larger than the expected seismic noise at the sites.

Details of these measurements are reported in [T1000738 SLC Suspension, Magnetic Field Measurements of the Eddy Current Damper](#).

3.2.3 LASTI Arm Cavity Baffle Suspension Test

The Arm Cavity Baffle Suspension, with a representative dummy load, was installed in the LASTI BSC chamber to test the effect of the baffle suspension internal modes on the transfer function of the ISC control system. The test results are described in

[T1000737 Stray Light Control Suspension, Results of the LASTI Test](#)

The measurement performed at LASTI on the SLC suspension attached to the ISI stage 0 with adequate damping of the rigid body modes, shows that the Arm Cavity Baffle suspension does not compromise the performance of the ISI Stage 0.

3.3 ALS Photo detector Array

A vacuum compatible ALS photodiode array is placed around the circumference of the Arm Cavity Baffle holes. The photodiodes will be used for lock acquisition by assisting in the initial pointing of the Power Recycling Cavity beam and the ALS beams.

The photo detector assemblies in their housings are mounted to the back side of the baffle, as shown in Figure 9, using stainless steel flat head screws that are visible from the beam side, with an opening in the baffle that allows only the active photo detector surface to be in the line of sight of the light from the far arm. Electrical cabling attaches to each photo detector, and electrical voltage and signals are carried through the cable to vacuum feed through that allow a connection to racks outside the vacuum chamber.

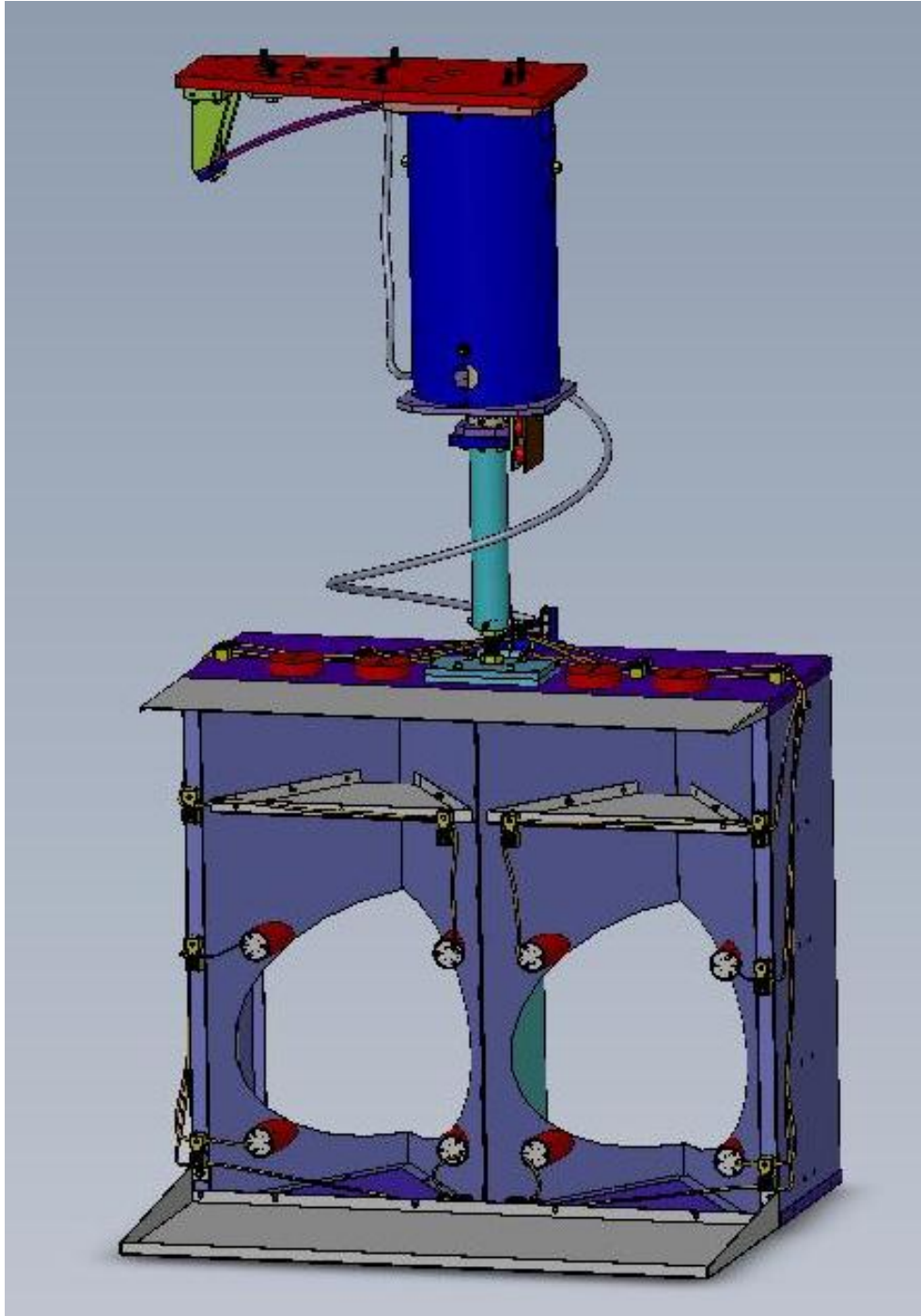


Figure 9: ALS Photodiodes Mounted to Back Side of ACB

The detail of the photo detector assembly is shown in Figure 10.

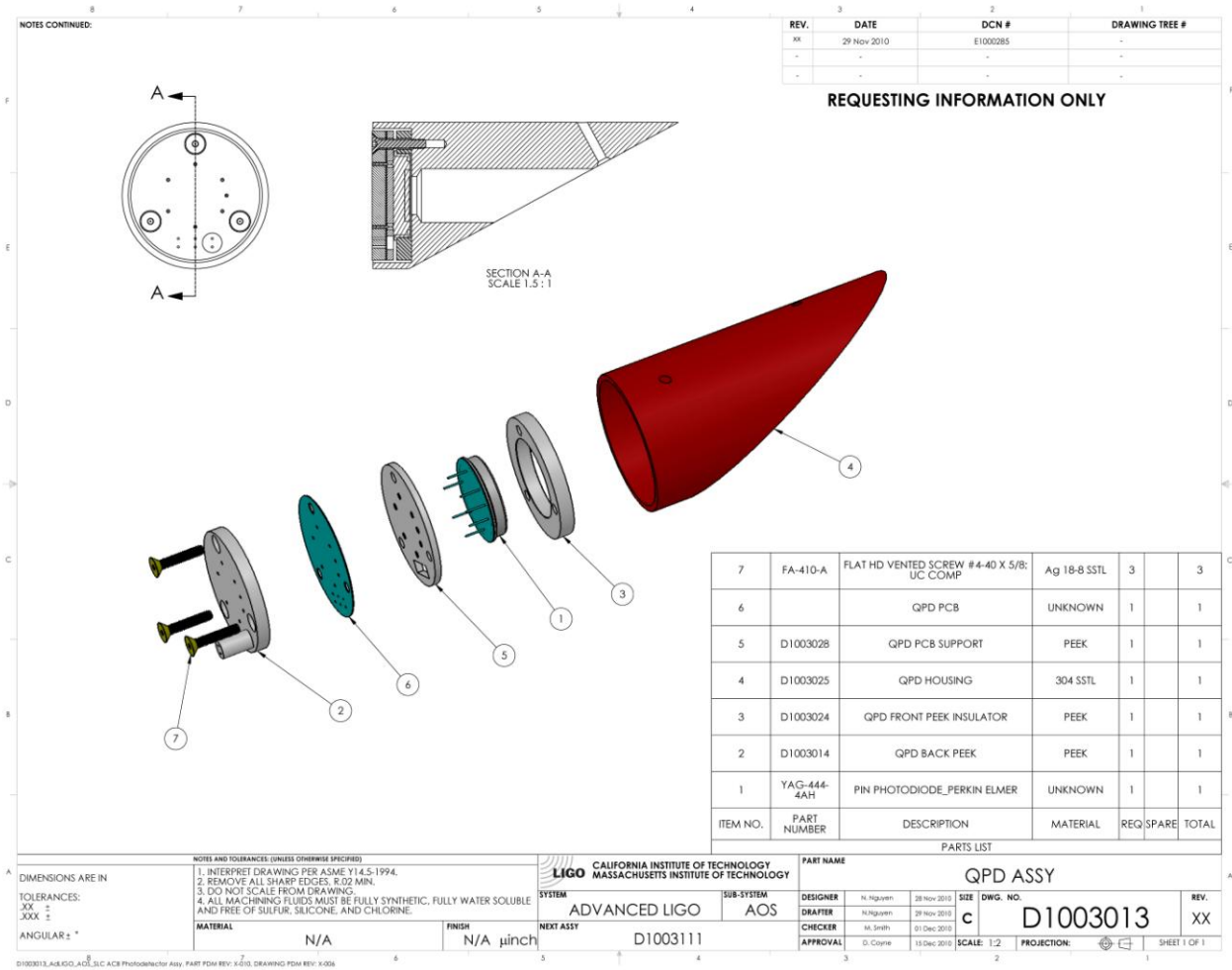
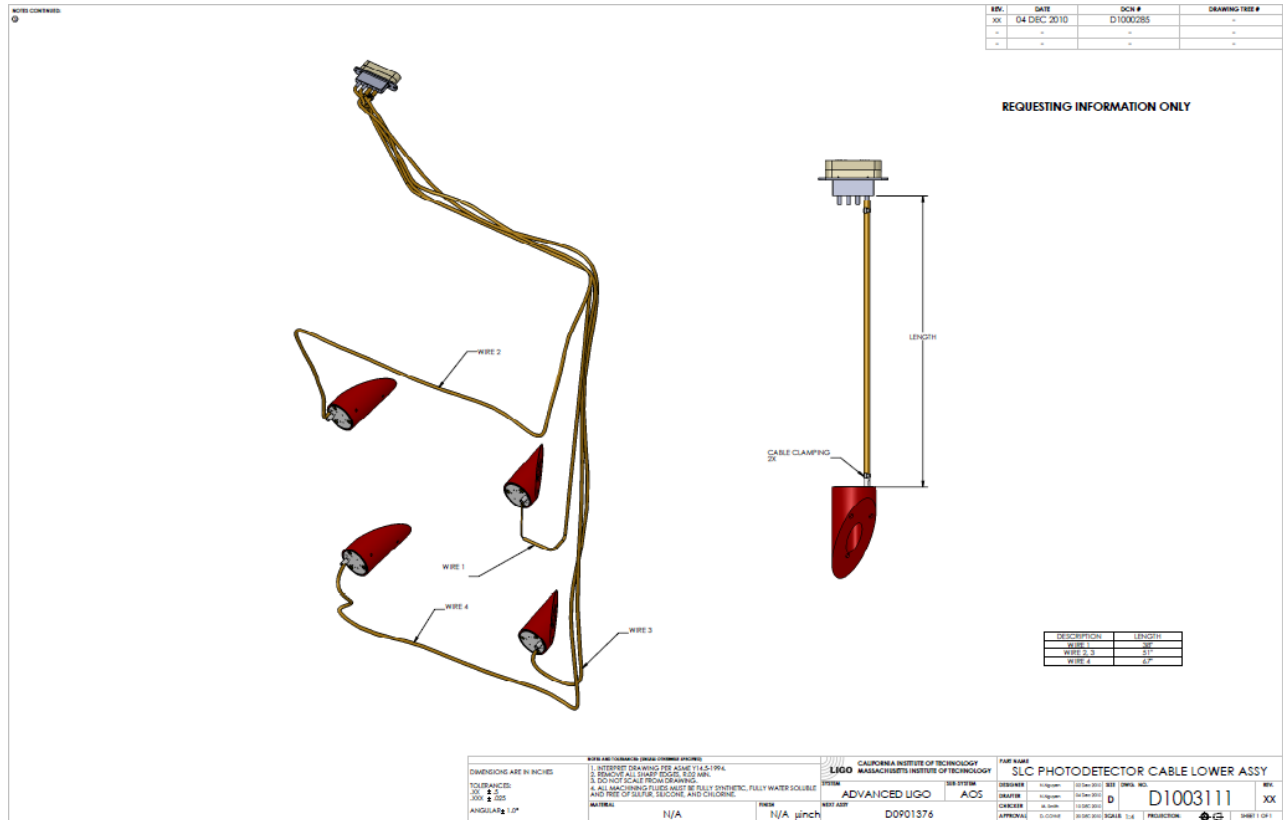


Figure 10: ALS Photo detector Assembly



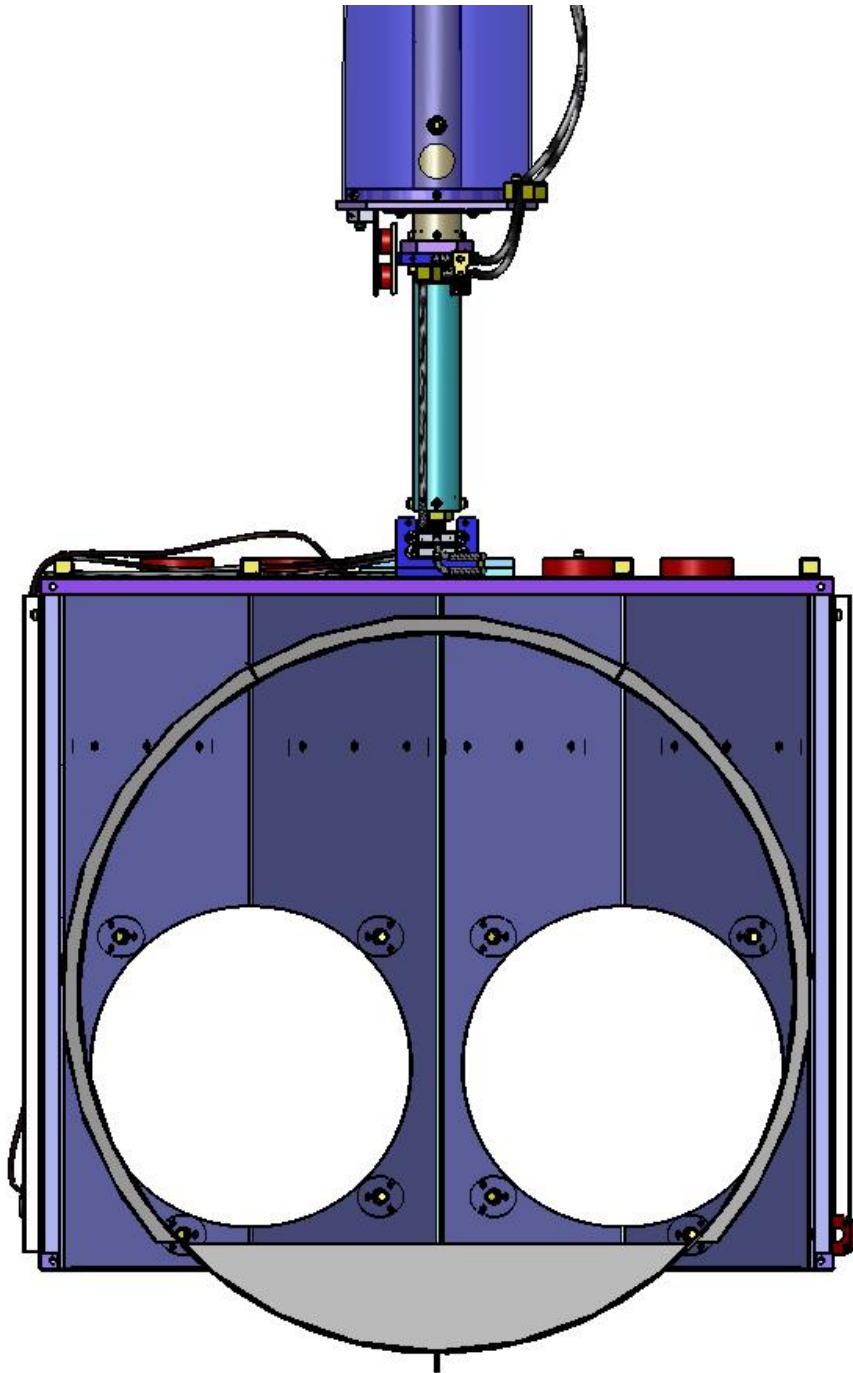


Figure 12: View toward the ALS Photo detector Array through the Manifold Cryopump Baffle Aperture

4 SCATTERED LIGHT DISPLACEMENT NOISE

The displacement noise caused by light scattering from the surface of the Arm Cavity Baffle, from the photo detector surface, and the surfaces of the fastening hardware is calculated in the following.

4.1 Arm Cavity Baffle Surface

The Arm Cavity Baffle Surface is black porcelainized steel, with an estimated BRDF $< 1E-4 \text{ sr}^{-1}$ (This value will be confirmed by measurement)--the measured BRDF of polished SS @ 50 deg incidence is $< 1E-4 \text{ sr}^{-1}$, and the measured BRDF of Black Glass is $< 1E-6$ --ref T080064. The parameters for the scattered light calculations are listed in [T0900269 Stray Light Control \(SLC\)](#)

4.1.1 Arm Cavity Baffle Surface Scatter

The small angle scattered power from the far arm cavity mirror passes through the beam tube to the near arm cavity mirror. The power in the annulus between the cryopump baffle and the ITM (ETM) outside diameter will hit the Arm Cavity Baffle. See Figure 13.

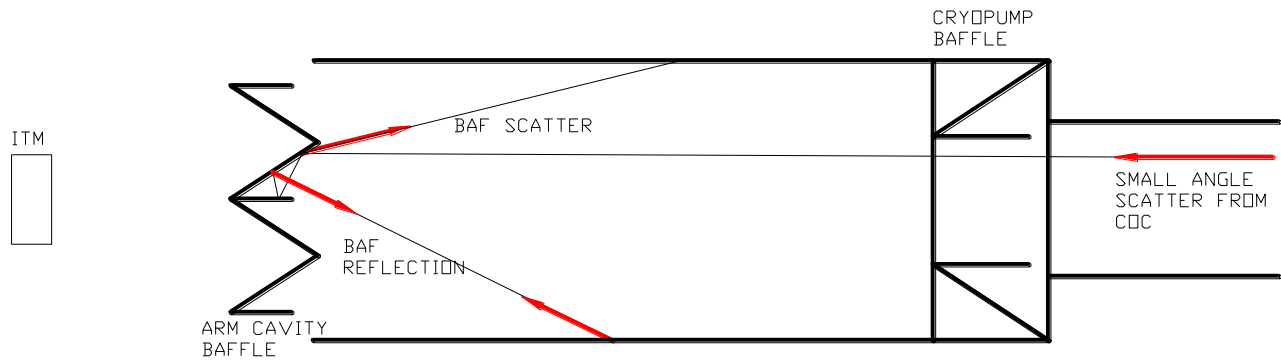


Figure 13: ARM CAVITY BAFFLE SCATTER

The offset between the arm cavity mirror and the beam tube axis will be ignored.

$$P_{acb} := P_a \cdot \int_{\theta_{ac}}^{\theta_{cp}} 2 \cdot \pi \cdot \theta \cdot BRDF_1(\theta) d\theta$$

The half-angle from the beam tube centerline to the AC baffle inner edge is

$$\theta_{ac} := \frac{R_{ac}}{L}$$

The half-angle from the beam tube centerline to the cryopump baffle outer edge is

$$\theta_{cp} := \frac{R_{cp}}{L}$$

P_a is the circulating power in each arm.

The light power scattered from four Arm Cavity Baffles into the mode cross section and re-scattered by the far COC into the IFO mode is given by

$$P_{\text{acbfafs}} := \sqrt{4} \cdot P_{\text{acb}} \cdot \text{BRDF}_{\text{bd}} \cdot \frac{\pi \cdot w_{\text{ifo}}^2}{L^2} \cdot \text{BRDF}_1 (30 \cdot 10^{-6}) \cdot \Delta_{\text{ifo}}$$

The scattering surface is suspended from the BSC ISI Stage 0 ring and has imposed on it the measured seismic motion in the beam direction, attenuated by the measured transmissibility of the Arm Cavity Baffle suspension.

The motion spectrum of the ISI State 0 ring is shown in Figure 14: Measured BSC ISI Stage 0, LLO.

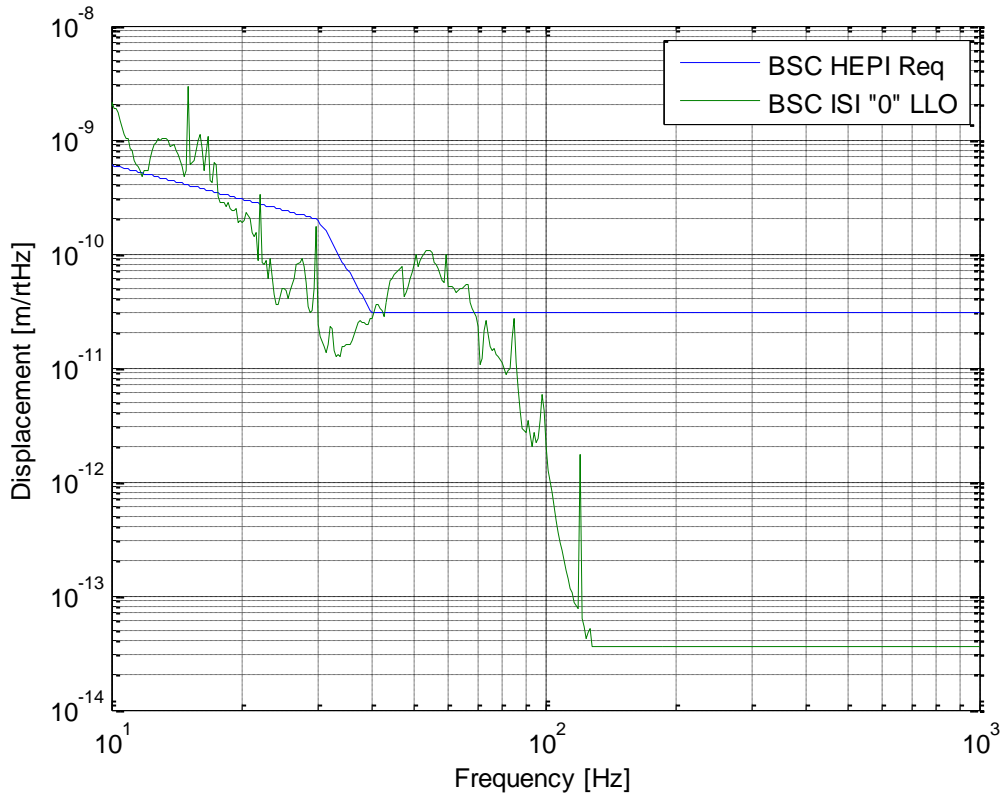


Figure 14: Measured BSC ISI Stage 0, LLO

The scattered light is injected into the arm cavity, and the appropriate scattered light noise transfer function is 'ITM_HR'. The displacement noise (m/rHz) is

$$\text{DN}_{\text{acbfaf}} := \text{TF}_{\text{itmhr}} \left(\frac{P_{\text{acbfafs}}}{P_{\text{psl}}} \right)^{0.5} \cdot x_{\text{hepi}} \cdot 2 \cdot k \cdot \text{acbatter}$$

4.2 Scattered Light Displacement Noise from ALS Photo detector Array

The photo detector surfaces and the heads of the mounting screws will scatter the main beam and the COC scattered light beam from the far end of the beam tube. The displacement noise caused by these scattering sources is two orders of magnitude less than that of the Arm Cavity Baffle surface.

4.3 Scattered Light Calculation Parameters

laser wavelength, m	$\lambda := 1.06410^{-6}$
wave number, m ⁻¹	$k := 2 \cdot \frac{\pi}{\lambda}$
	$k = 5.9052 \times 10^6$
IFO waist size, m	$w_{\text{ifo}} := 0.01$
solid angle of IFO mode, sr	$\Delta_{\text{ifo}} := \frac{\lambda^2}{\pi \cdot w_{\text{ifo}}^2}$
	$\Delta_{\text{ifo}} = 2.5025 \times 10^{-9}$
Transfer function @ 100 Hz, ITM HR	$TF_{\text{itmhr}} := 1.1 \cdot 10^{-9}$
Gaussian beam radius at ITM, m	$w := 0.05$
IFO arm length, m	$L_{\text{ifo}} := 400$
PSL laser power, W	$P_{\text{psl}} := 12$
Arm Power, W	$P_0 := 83417$
BRDF, sr ⁻¹ ; CSIRO, surface 2, S/N 2	$BRDF_1(\theta) := \frac{2755.12}{(1 + 8.5078710^8 \cdot \theta^2)^{1.23597}}$
BRDF_porcelain_ss	$BRDF_{\text{porc}} := 2 \cdot 10^{-3}$
BRDF of photo detector, sr ⁻¹	$BRDF_{\text{pd}} := 1 \cdot 10^{-3}$
BRDF of screw head sr ⁻¹	$BRDF_{\text{sh}} := 5 \cdot 10^{-2}$

BRDF_COC_30urad, sr ⁻¹	$BRDF_{COC} := BRDF_1(30 \cdot 10^{-6})$	
	$BRDF_{COC} = 1.3644 \times 10^3$	
number of photo detector	$N_{pd} := 1\epsilon$	
number of screw heads	$N_{sh} := 4\epsilon$	
radius of photo detector ring, m	$r_{pdbc} := 0.19\epsilon$	
Photoconductor radius, m	$r_{pd} = 5.7 \times 10^{-3}$	
photoconductor area, m ²	$A_{pd} := \pi \cdot r_{pd}^2$	$A_{pd} = 1.0207 \times 10^{-4}$
Screw head radius, m	$r_{sh} := .003\epsilon$	
Screw head area, m ²	$A_{sh} := \pi \cdot r_{sh}^2$	$A_{sh} = 4.5365 \times 10^{-5}$

4.4 Scattering from Main Arm Beam

4.4.1 Power Hitting Photo detector Surface and Screw Head

irradiance function at ACB, W/m ²	$I_{pd}(r) := 2 \cdot \frac{P_0}{\pi \cdot w^2} \cdot e^{-2 \cdot \left(\frac{r^2}{w^2}\right)}$
total beam power, W	$P_0 := \int_0^{10w} 2 \cdot \pi \cdot r \cdot I_{pd}(r) dr$
	$P_0 = 8.3417 \times 10^5$
Irradiance at photo detector, W/m ²	$I_{pd}(r_{pdbc}) = 1.6359 \times 10^{-3}$

Power hitting each PD, W

$$P_{pd} := I_{pd}(r_{pdbc}) \cdot A_{pd}$$

$$P_{pd} = 1.6698 \times 10^{-7}$$

Power hitting each screw head, W

$$P_{sh} := I_{pd}(r_{pdbc}) \cdot A_{sh}$$

$$P_{sh} = 7.4213 \times 10^{-8}$$

4.4.2 Power Scattered into IFO Mode

half-angle from centerline to inner edge of PD, rad

$$\theta_{pdi} := \frac{(r_{pdbc} - r_{pd})}{L}$$

half-angle from centerline to outer edge of PD, rad

$$\theta_{pdo} := \frac{(r_{pdbc} + r_{pd})}{L}$$

average angle, rad

$$\theta_{pd} := \frac{\theta_{pdi} + \theta_{pdo}}{2}$$

$$\theta_{pd} = 4.9 \times 10^{-5}$$

BRDF at photo detector, angle, sr⁻¹

$$\text{BRDF}_1(4.9 \times 10^{-5}) = 696.3695$$

4.4.2.1 Scattering by Photo detector

power scattered by photo detector,
into IFO mode, W

$$P_{pds} := \sqrt{N_{pd}} \cdot P_{pd} \cdot \text{BRDF}_{pd} \cdot \frac{\pi \cdot w_{ifo}^2}{L^2} \cdot \text{BRDF}_1(4.9 \times 10^{-5}) \cdot \Delta_{ifo}$$

$$P_{pds} = 3.291 \times 10^{-26}$$

4.4.2.2 Scattering by Screw Head

power scattered by screw head
into IFO mode, W

$$P_{\text{shs}} := \sqrt{N_{\text{sh}}} \cdot P_{\text{sh}} \cdot \text{BRDF}_{\text{sh}} \cdot \frac{\pi \cdot w_{\text{ifo}}^2}{L^2} \cdot \text{BRDF}_1(4.9 \times 10^{-5}) \cdot \Delta_{\text{ifo}}$$

$$P_{\text{shs}} = 1.2667 \times 10^{-24}$$

4.4.3 Displacement Noise

ACB displacement @ 100 HZ, m/rt HZ $x_{\text{ACB}} := 1 \cdot 10^{-12}$

displacement noise @ 100 Hz, m/rtHz $\text{DN}_{\text{acbpd}} := \text{TF}_{\text{itmhr}} \left(\frac{P_{\text{pds}}}{P_{\text{psl}}} \right)^{0.5} \cdot x_{\text{ACB}}^{2 \cdot k}$

$$\text{DN}_{\text{acbpd}} = 2.108 \times 10^{-28}$$

4.5 Scattering from COC Scattered Light

4.5.1 Power Hitting Photo detector Surface and Screw Head

COC Scattered power hitting the PD, W $P_{\text{cocpd}} := P_0 \cdot \text{BRDF}_1(\theta_{\text{pd}}) \cdot \frac{A_{\text{pd}}}{L^2} = 3.7057 \times 10^{-3}$

COC Scattered power hitting
the screw head W $P_{\text{cocsh}} := P_0 \cdot \text{BRDF}_1(\theta_{\text{pd}}) \cdot \frac{A_{\text{sh}}}{L^2} = 1.647 \times 10^{-3}$

4.5.2 Power Scattered into IFO Mode

4.5.2.1 Scattering by Photo detector

power scattered by photo detector,
into IFO mode, W

$$P_{\text{cocpds}} := \sqrt{N_{\text{pd}}} \cdot P_{\text{cocpd}} \cdot \text{BRDF}_{\text{pd}} \cdot \frac{\pi \cdot w_{\text{ifo}}^2}{L^2} \cdot \text{BRDF}_1(4.9 \times 10^{-5}) \cdot \Delta_{\text{ifo}}$$

$$P_{\text{cocpds}} = 7.3036 \times 10^{-22}$$

4.5.2.2 Scattering by Screw Head

power scattered by screw head
into IFO mode, W

$$P_{\text{cocshs}} := \sqrt{N_{\text{sh}}} \cdot P_{\text{cocsh}} \cdot \text{BRDF}_{\text{sh}} \cdot \frac{\pi \cdot w_{\text{ifo}}^2}{L^2} \cdot \text{BRDF}_1(4.9 \times 10^{-5}) \cdot \Delta_{\text{ifo}}$$

$$P_{\text{cocshs}} = 2.8112 \times 10^{-20}$$

4.5.3 Displacement Noise

displacement noise @ 100 Hz, m/rtHz

$$\text{DN}_{\text{cocpd}} := \text{TF}_{\text{itmhr}} \left(\frac{P_{\text{cocpds}}}{P_{\text{psl}}} \right)^{0.5} \cdot x_{\text{ACB}}^{2 \cdot k}$$

$$\text{DN}_{\text{cocpd}} = 3.1403 \times 10^{-26}$$

$$\text{DN}_{\text{cocsh}} := \text{TF}_{\text{itmhr}} \left(\frac{P_{\text{cocshs}}}{P_{\text{psl}}} \right)^{0.5} \cdot x_{\text{ACB}}^{2 \cdot k}$$

$$\text{DN}_{\text{cocsh}} = 1.9483 \times 10^{-25}$$

The full scattering displacement noise spectrum is shown in Figure 15, and is compared with the AOS requirement.

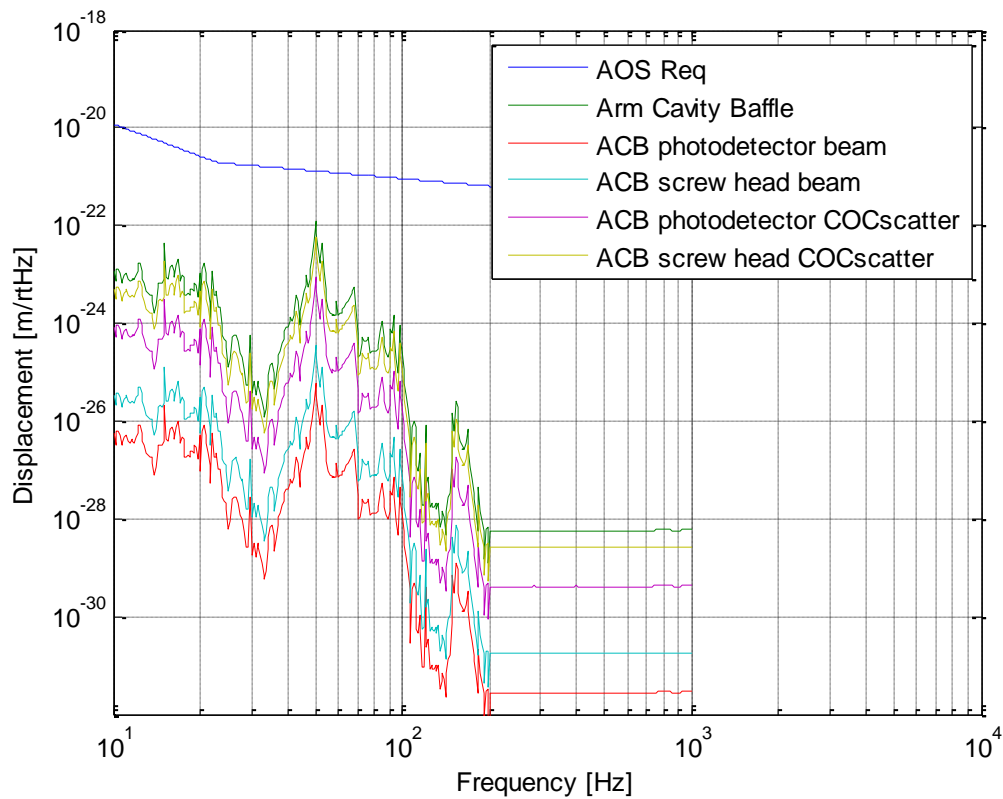


Figure 15: Scattered Light Displacement Noise from Arm Cavity Beam, and from the COC Scattered Light

5 INTERFACES

5.1 Installation of the Arm Cavity Baffle in the BSC Chamber

The suspension assembly for the Arm Cavity Baffle will be installed on ISI Stage 0 while it is on the Cartridge prior to insertion into the BSC Chamber, as shown in Figure 16.

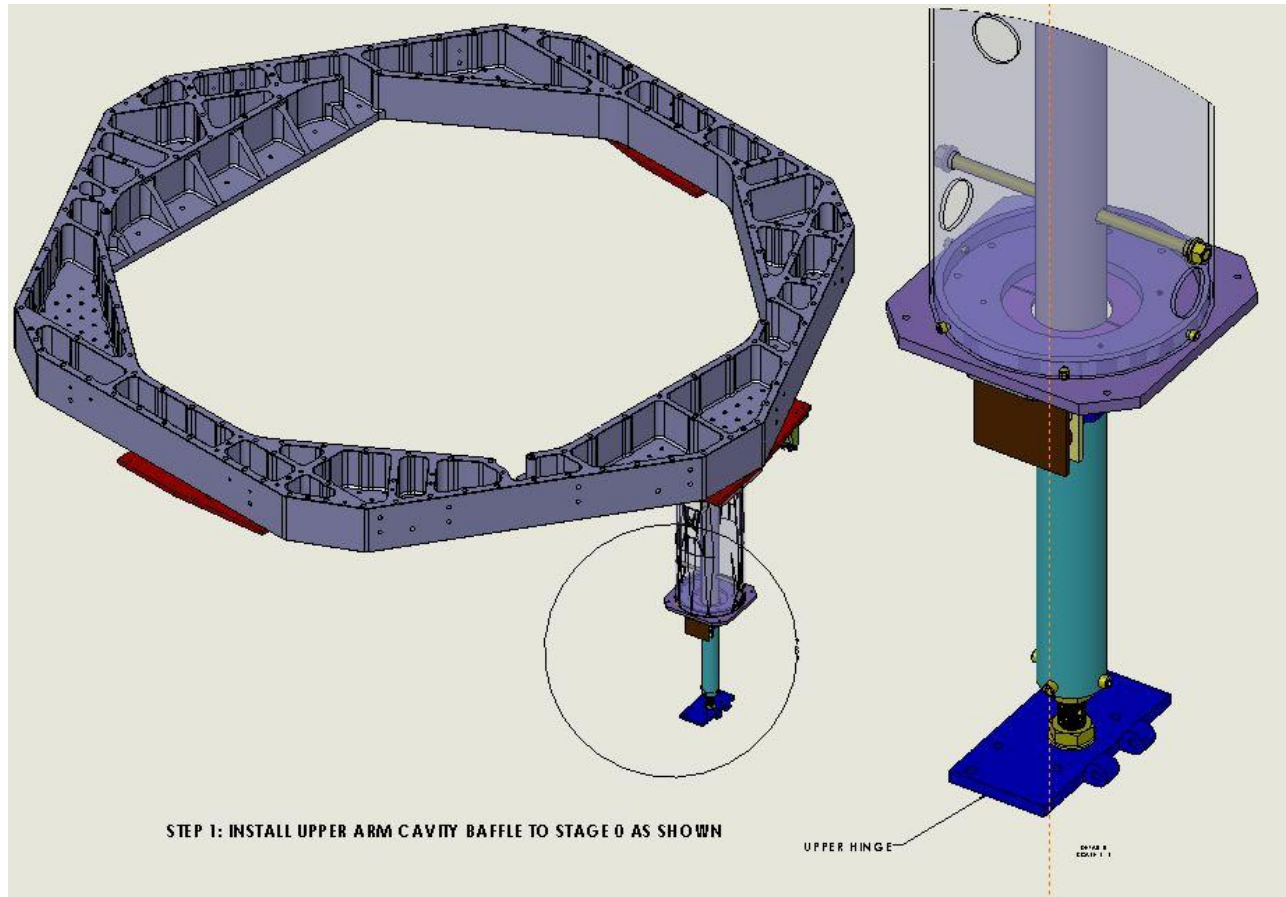


Figure 16: Installation of Arm Cavity Baffle Suspension Assembly while in the Cartridge

Once the ISI Stage 0 has been inserted into the BSC chamber, and after the Quad Suspensions have been installed, the lower portion of the Arm Cavity Baffle will be brought into the BSC chamber and attached to the upper hinge, as shown in

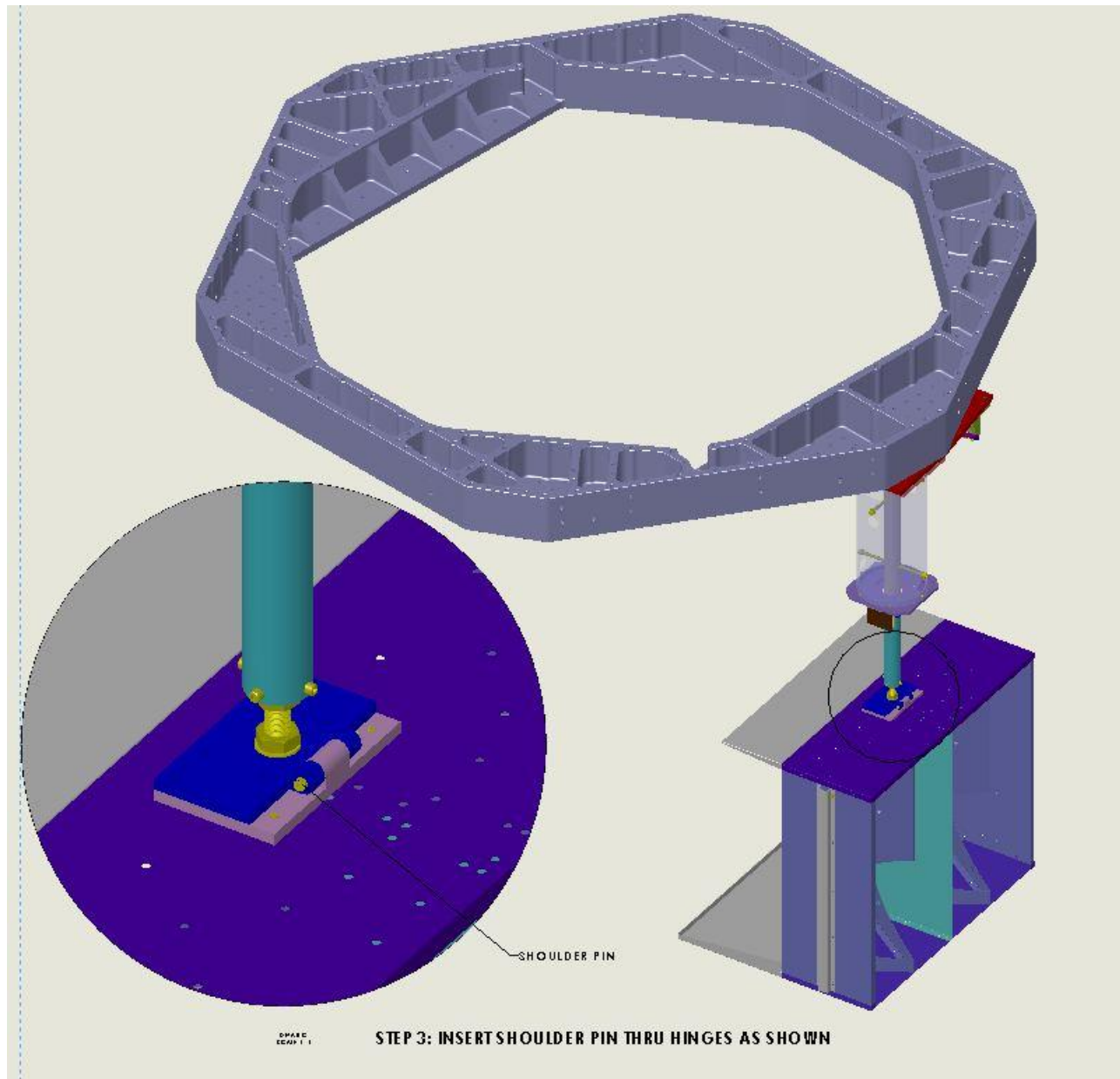


Figure 17: Attachment of Lower Arm Cavity Baffle Assy to the Suspension

5.2 Interface to ITM and ETM Mirrors

The Arm Cavity Baffle meets the requirement of giving access to the ITM and ETM mirrors and suspension by being hinged out of the way, as described in 3.1.1. The distance between the baffle and the quad suspension frame before hinging away is given in the following document:

[E1000404-v1 ACB Interface in BSC Chambers H1, H2 for Advanced LIGO\(2\)](#)

A Solid Works drawing of the Arm Cavity Baffle in its installed position in BSC 8 is shown in Figure 19.

5.3 Interface to ISI Stage 0

The Arm Cavity Baffle suspension support plate is attached to the ISI Stage 0 by means of clamps fastened with bolts into the threaded holes of the Stage 0. The locations of the support plate on the ISI Stage 0 for the various BSC chambers is shown in Figure 18.

One lesson learned from the Arm Cavity Baffle suspension test at LASTI is that the support plate should be clamped as close as possible to the down tube of the suspension structure to avoid resonances due to cantilever flexing of the support plate.

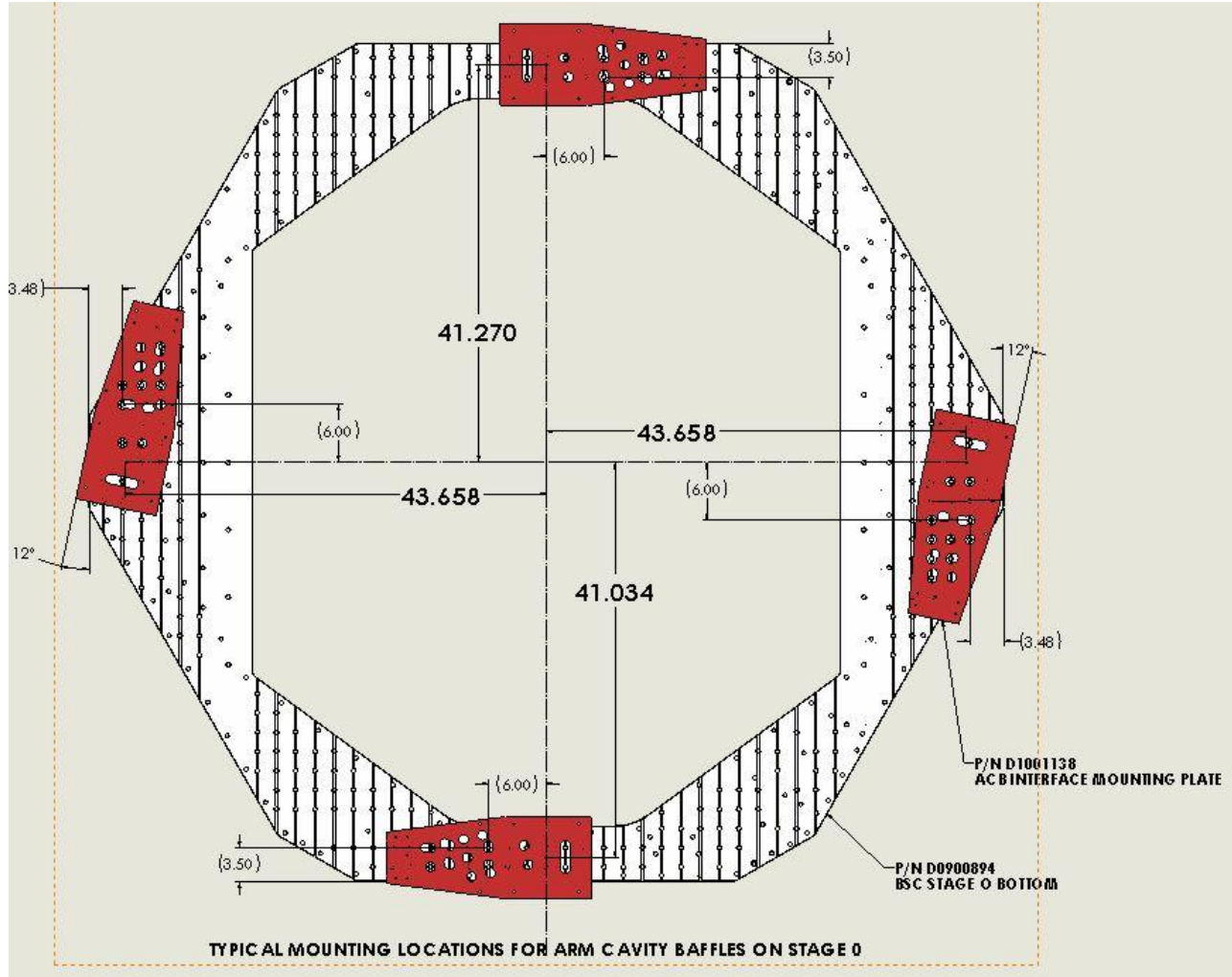


Figure 18: Mounting locations of the Arm Cavity Baffle in the Various BSC Chambers.

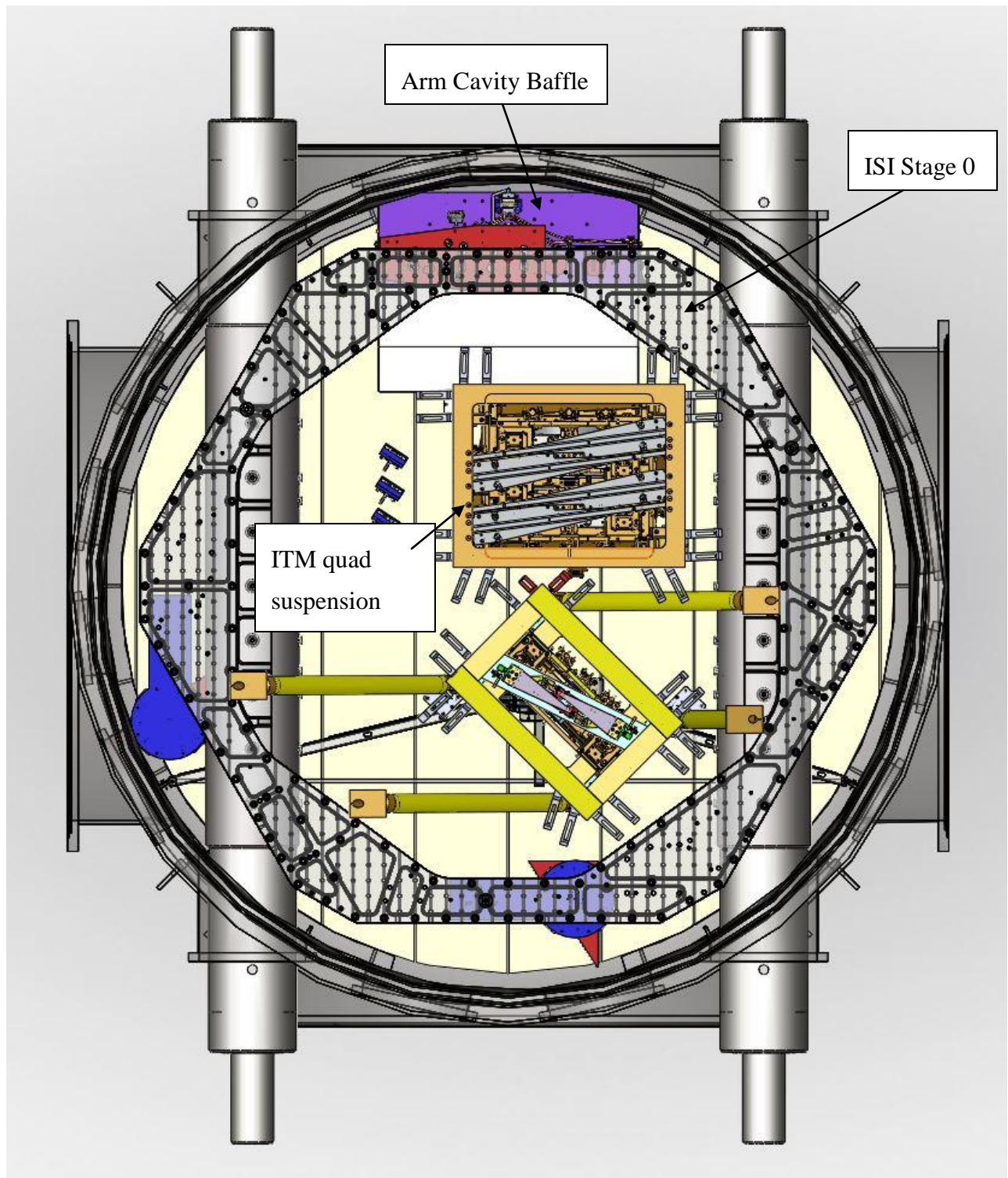


Figure 19: Arm Cavity Baffle Installed in BSC8

The Figure 20 shows the detail of the Arm Cavity Baffle suspension support plate clamped to the Stage 0; the support plate has been made transparent so that the down tube mounting plate and other details of the baffle suspension that hang below the transparent suspension support plate can be seen. In particular, a mounting access slot is located near the center of the down tube where a clamp can be positioned to minimize the bending of the suspension support plate due to the weight of the down tube assembly; other clamps attach to available mounting holes in the Stage 0.

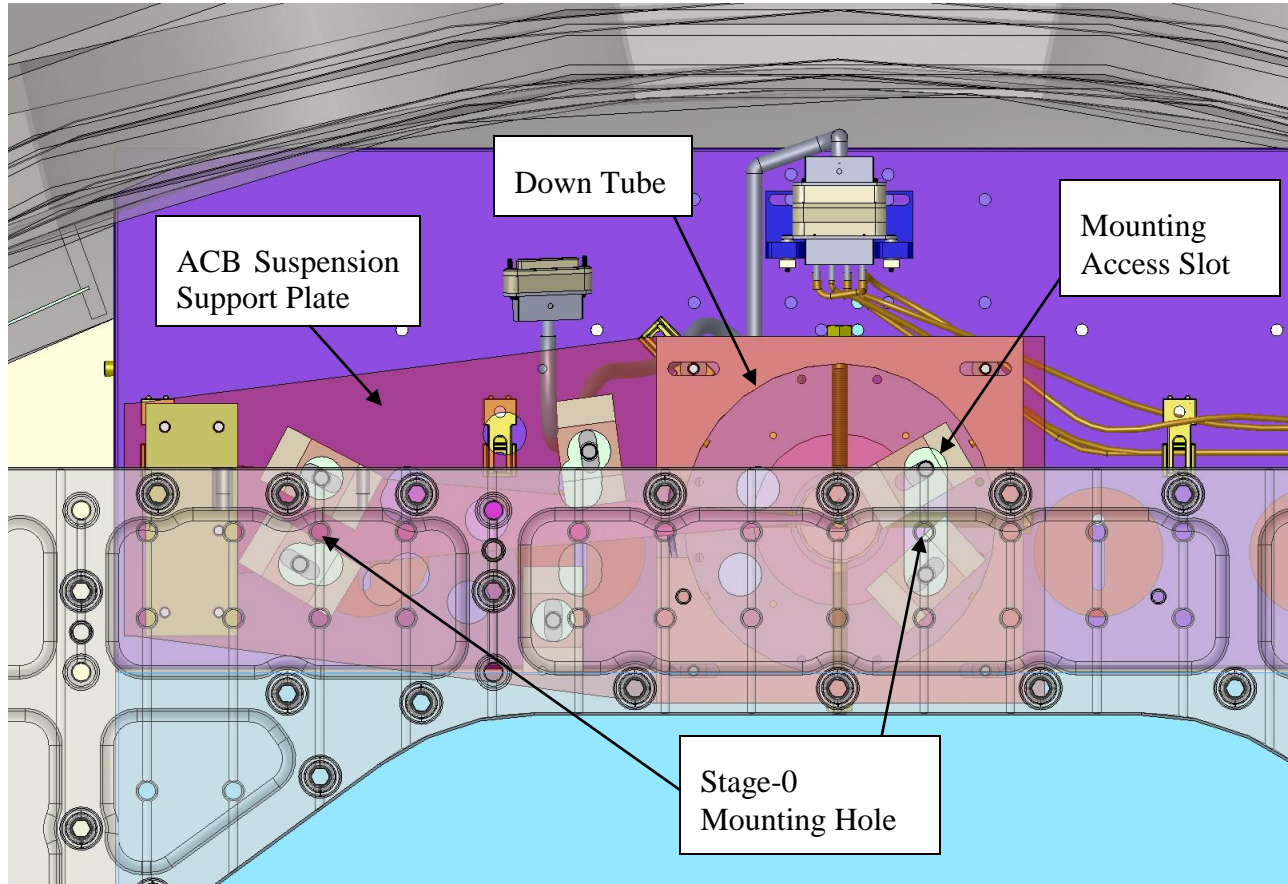


Figure 20: Detail of Arm Cavity Attachment to Stage 0

Further detail of the clamping arrangement is shown in Figure 21.

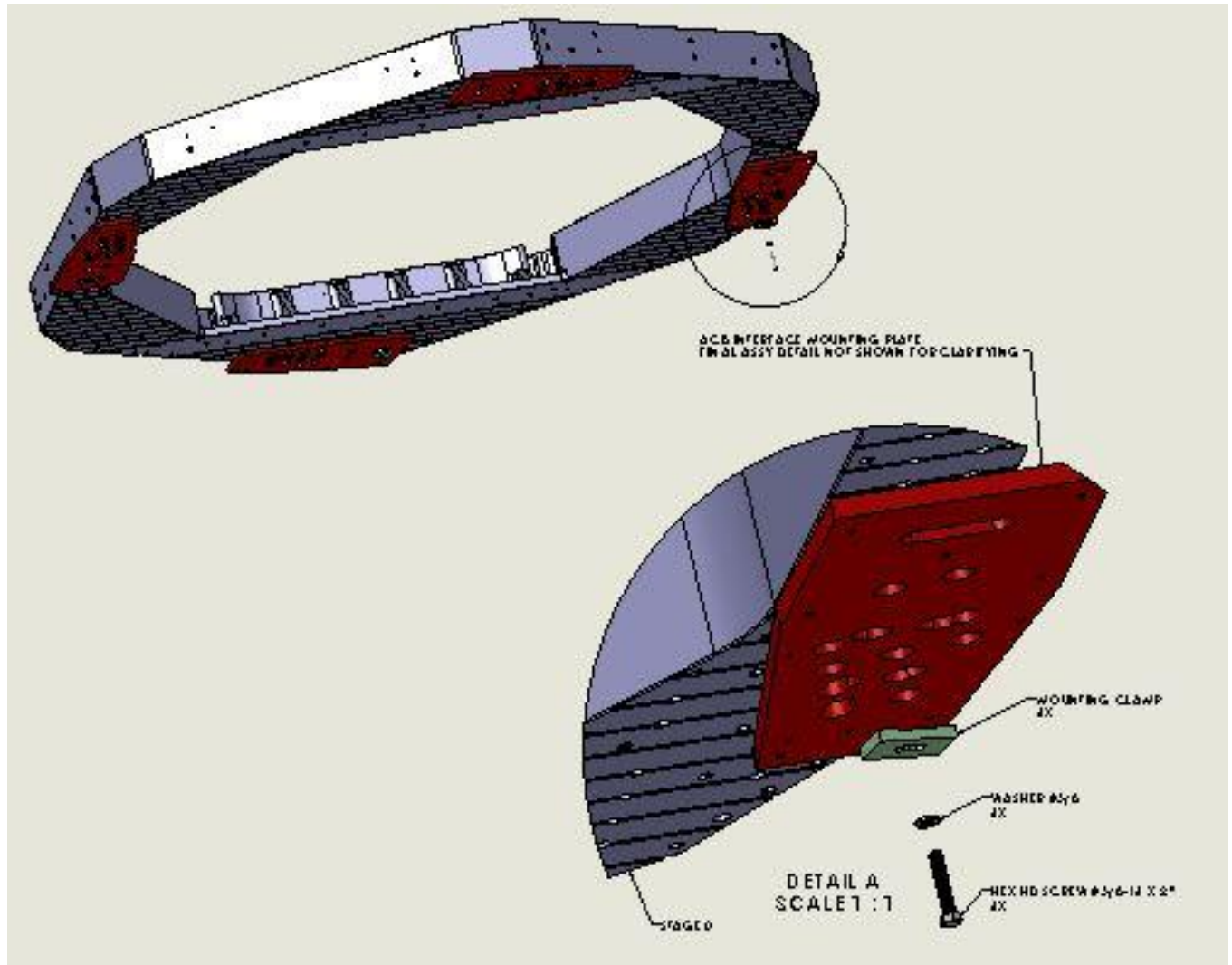


Figure 21: Detail of support plate clamp attachment

5.4 Stay Clear Margin

The aperture of the Arm Cavity Baffle is 346 mm, which is larger than the 340 mm diameter of the ITM and ETM COC, and the ACB will not cause a power loss of the arm cavity beam. The aperture will be aligned concentric to the COC within 4 mm.

5.5 Electrical Interfaces

The ALS photo detector electrical power and signal cables will be terminated at the internal vacuum feed through in the BSC chamber, as described in [D1002870, Flange Layout, Cable Lengths, Bracket Location and Related Input Documents](#). The internal feed through connection is the interface between AOS and ISC--AOS is not responsible for cabling outside the vacuum chamber